

Supplementary information

Synthesis, Antitumor Activity, 3D-QSAR and Molecular Docking Studies of New Iodinated 4-(3*H*)-quinazolinones 3*N*-substituted

Marcia Pérez-Fehrmann^a, Víctor Kesternich^a, Arturo Puelles^a, Víctor Quezada^a, Fernanda Salazar^a, Philippe Christen^b, Jonathan Castillo^c, Juan Guillermo Cárcamo^{c,d}, Alejandro Castro-Alvarez^{e,f}, Ronald Nelson^{a*}.

^a *Departamento de Química, Facultad de Ciencias, Universidad Católica del Norte, Casilla 567, Antofagasta, Chile.*

^b *School of Pharmaceutical Sciences, University of Geneva, University of Lausanne, Rue Michel-Servet 1, CH-1211 Geneva 4, Switzerland.*

^c *Instituto de Bioquímica y Microbiología, Facultad de Ciencias, Universidad Austral de Chile, Campus Isla Teja, Valdivia, Chile.*

^d *Centro FONDAP, Interdisciplinary Center for Aquaculture Research (INCAR), Chile.*

^e *Laboratorio de bioproductos farmacéuticos y cosméticos, Centro de Excelencia en Medicina Traslacional, Facultad de Medicina, Universidad de La Frontera, Av. Francisco Salazar 01145, Temuco, 4780000, Chile.*

^f *Departamento de Química de los Materiales, Facultad de Química y Biología, Universidad de Santiago de Chile, Casilla 40, Correo 33, Santiago, Chile.*

*Corresponding Author E-mail: rnelson@ucn.cl

Contents

1. General.....	2
2. Cytotoxicity assay.....	4
3. Pathak's structures for 3D-QSAR study.....	20
4. Principal spectroscopy data	21
5. ¹ H NMR and ¹³ C-APT NMR spectra of compounds.....	22

1. General

Synthesis: Melting points were determined on a Kofler-type apparatus and were uncorrected. The IR spectra were taken on a Perkin-Elmer 200 spectrophotometer with KBr. NMR spectra were collected in DMSO- d_6 or CD₃OD with a Varian Unity Inova 500 MHz spectrometer. Chemical shifts were reported in parts per million (δ) using the residual solvent signals (DMSO- d_6 : δ_H 2.50, δ_C 39.5 or CD₃OD; δ_H H 3.31, δ_C C 49.0) as the internal standards for the ¹H and ¹³C NMR spectra and coupling constants (J) in Hz. HRMS spectra were recorded on a Micromass-LCT Premier Time-of-Flight ESI spectrometer with an Acquity Ultra-high-performance liquid chromatography interface system. TLC was performed on Si gel Merck 60 F₂₅₄ (Al plates) and the TLC plates were visualized by spraying with phosphomolybdic acid reagent and heating. The starting materials and reagents were purchased from Sigma–Aldrich or Merck and used without further purification.

Cytotoxicity assay: Human gallbladder adenocarcinoma (G415), human gallbladder adenocarcinoma (Gbd1), human promyelocytic leukemia (HL60), human histiocytic lymphoma (U937), human cervix adenocarcinoma (HeLa) and human brain glioblastoma multiforma (T98G) cell lines were purchased from the American Type Culture Collection (Manassas, VA, USA). All cell lines were grown at 37 °C in a humidified atmosphere of 5% CO₂ environment and the adherent cells were removed from culture plates by trypsinization (0.5 mM EDTA, 0.05% trypsin). G-415 and Gbd1 were maintained in RPMI 1640 supplemented with 2 mM glutamine, 10% FBS, penicillin/streptomycin/amphotericin-B (100 units/ml; 100 µg/ml; 0.25 µg/ml). Confluent cultures of these two adherent cell lines were split 1:3 to 1:6 by trypsinization and seeded at 2-4x10⁴ cells/cm². HL60 and U937 cells were grown in the same medium and seeded at 1-5x10⁵ and 2-9 x10⁵ cells/mL, respectively. Three times per week, the culture cells were diluted under the same conditions to maintain density and were harvested in the exponential phase of growth. HeLa cells were cultured in MEM, containing 2 mM glutamine, 10% FBS, 1% non-essential amino acids, penicillin/streptomycin/amphotericin-B (100 units/mL; 100 µg/mL; 0.25 µg/mL). T98G cells were grown in DMEM-F12 supplemented with 2 mM glutamine, 10% FBS, 1% non-essential amino acids, 1% sodium pyruvate, penicillin/streptomycin/amphotericin-B (100 units/mL; 100 µg/mL; 0.25 µg/mL). Confluent cultures of these last two adherent cell lines were split 1:3 to 1:6 by trypsinization and seeded at 2-4 x10⁴ cells/cm². For cytotoxicity studies, cells were seeded in a 96-well microtiter plate at a density of 5 x 10⁵/mL and allowed to adhere for 24 h in a CO₂ incubator. One day after seeding, cells were treated with fresh medium containing the compounds, dissolved in DMSO (1% final concentration in the well) plus culture medium, incubating by 24 h at 37 °C. The compound concentrations ranged from 0 µM up to 200 µM. After incubation, 10 µL aliquots of MTT solution (5 mg/mL in PBS) were added to each well and re-incubated for 4 h at 37 °C, followed by low centrifugation at 800 rpm for 5 minutes. Cell viability was determined by means of MTT reduction and the cells incubated in culture medium alone and 1% DMSO served as control for cell viability (untreated cells). 200 µL of supernatant was carefully aspirated and 200 µL aliquots of 100% DMSO were added to each well to dissolve the formazan crystals, followed by incubation of 10 minutes at 37 °C to dissolve air bubbles. The culture plate was placed on an *Emax* model micro-plate reader (Molecular Devices) and the absorbance was measured spectrophotometrically at 650 nm. The amount of color produced is directly proportional to

the number of viable cells. Untreated cells and the controls containing 1% DMSO were used as 100% viability controls. Paclitaxel (T7191, Sigma-Aldrich) was used as reference compound. All assays were performed twice with three replicates and processed independently. Mean \pm SD was used to estimate the cell viability. Cell viability rate was calculated as the percentage of MTT absorption as follows:

$$\% \text{ survival} = (\text{mean experimental absorbance} / \text{mean control absorbance}) \times 100$$

The compound concentration was plotted against the corresponding percentage (%) of cell viability obtained with MTT assays, and the 50% inhibitory concentration (IC_{50}) was calculated by non-linear regression. The curve fittings were performed using GraphPad Prism[®]6 from Systat Software, Inc. Compounds with $IC_{50} > 200 \mu\text{M}$ were considered as inactive.

Computational method: The preparations of iodinated 4-(3*H*)-quinazolinone 3D structures were obtained with OpenBabel¹ from SMILES annotations for each ligand. Protonation states were adjusted to pH 7.2 using FixpKa and AM1BCC charges implemented in the QUACPAC package,² followed by conformer generation using OMEGA.³ Docking was performed using FRED⁴ and the coordinates of the co-crystal structure of DFHR (PDB code 4M6J),⁵ keeping 20 poses for each docked molecule. Optimization of the docked poses was carried out using a two-step protocol and SZYBKI.⁶ First, optimization of the ligand's Cartesian coordinates was performed using a constraint of 1 kcal/mol, followed by optimization of the complex using MMFF94s as a force field, a Poisson–Boltzmann model, and AM1BCC charges for the ligands. Flexibility of residue side chains were kept within 6 Å of the ligand. The resulting poses were ranked according to the predicted ligand-protein energy, and the pose with the lowest score was selected as the best pose for each molecule.

3D-QSAR models were obtained with the Open3DQSAR package,⁷ which performs partial least squares (PLS) regression models from molecular interaction fields (MIF). Unless otherwise noted, default parameters were employed for Open3DQSAR. The input to Open3DQSAR is a set of aligned conformers of the dataset with associated bioactivities. A grid was constructed around the aligned molecules in such a way that its box exceeded 5 Å in the largest molecule, and grid spacing was set to 0.5 Å. Steric and electrostatic molecular mechanics of MIFs were computed using the Merck force field (MMFF94). The pictures were obtained with Chimera UCSF and PyMol software.

¹ N. M. O'Boyle, M. Banck, C. A. James, C. Morley, T. Vandermeersch and G. R. Hutchison, *Journal of Cheminformatics*, 2011, **3**, 1–14

² QUACPAC 2.0.1.2: OpenEye Scientific Software, Santa Fe, NM. <http://www.eyesopen.com>

³ P. C. D. Hawkins, A. G. Skillman, G. L. Warren, B. A. Ellingson and M. T. Stahl, *Journal of Chemical Information and Modeling*, 2010, **50**, 572–584.

⁴ M. McGann, *Journal of Chemical Information and Modeling*, 2011, **51**, 578–596.

⁵ G. Bhabha, D. C. Ekiert, M. Jennewein, C. M. Zmasek, L. M. Tuttle, G. Kroon, H. J. Dyson, A. Godzik, I. A. Wilson and P. E. Wright, *Nature Structural and Molecular Biology*, 2013, **20**, 1243–1249.

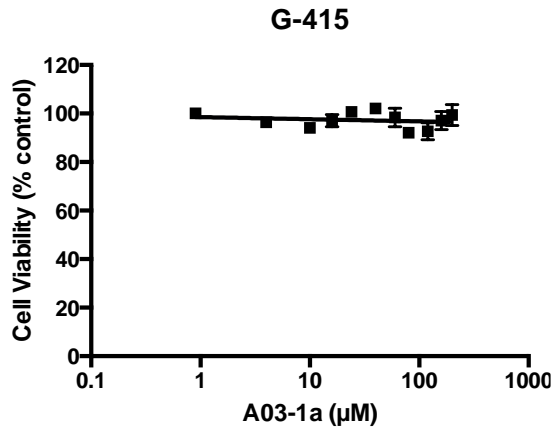
⁶ SZYBKI 1.10.1.2: OpenEye Scientific Software, Santa Fe, NM. <http://www.eyesopen.com>

⁷ P. Tosco and T. Balle, *Journal of Molecular Modeling*, 2011, **17**, 201–208.

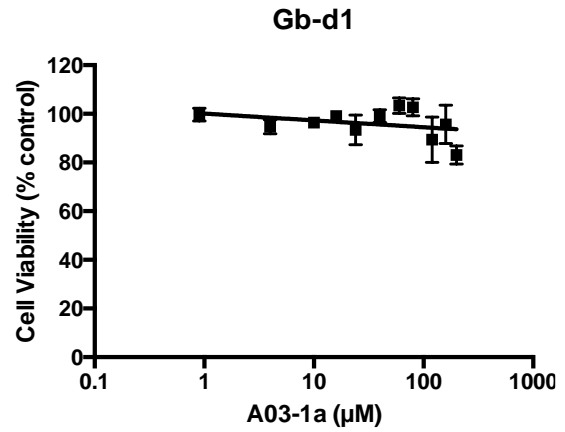
2. Cytotoxicity assay

3a

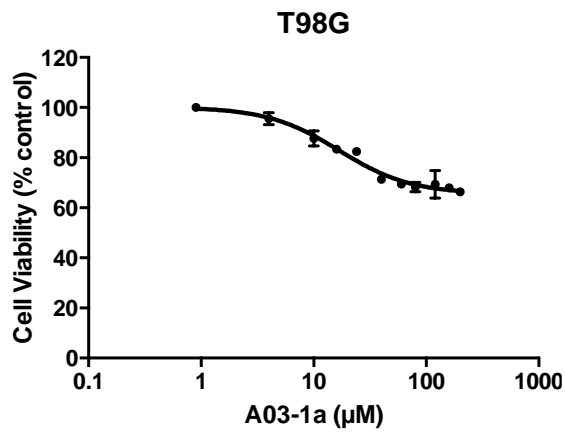
G-415



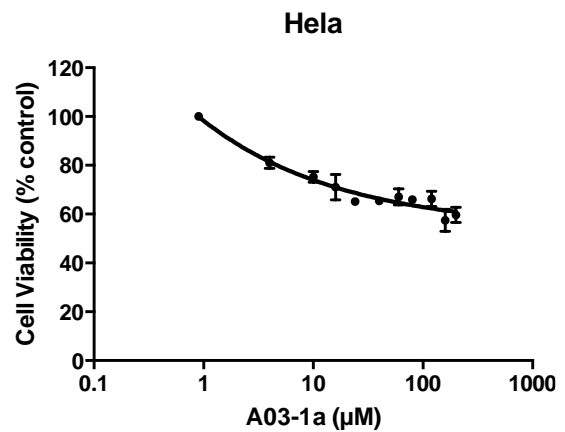
Gb-d1



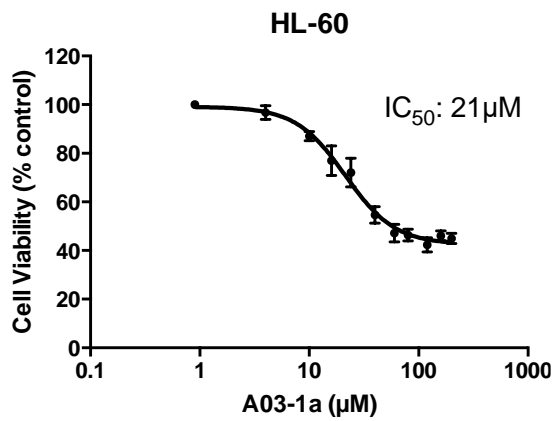
T98G



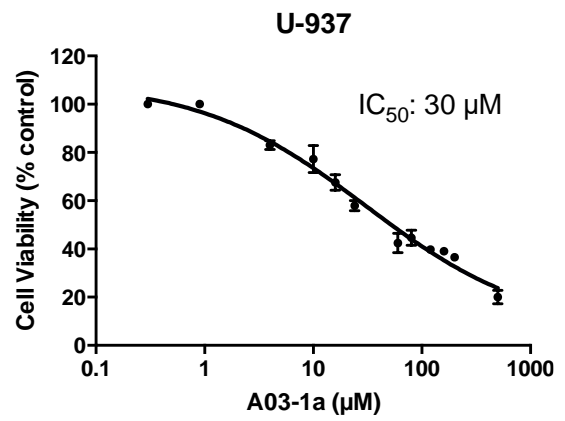
Hela



HL-60

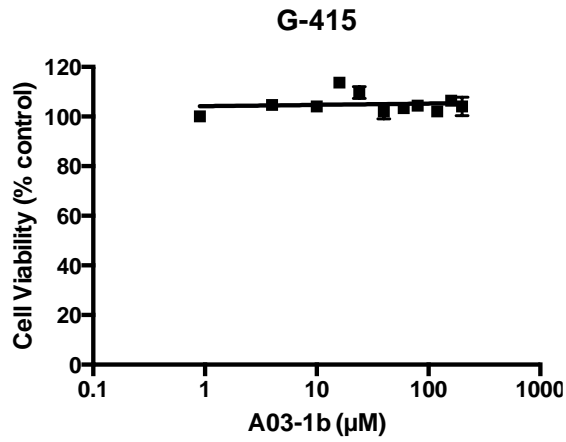


U-937

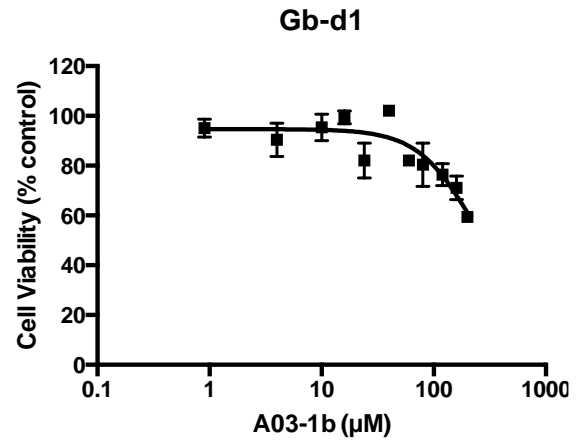


3b

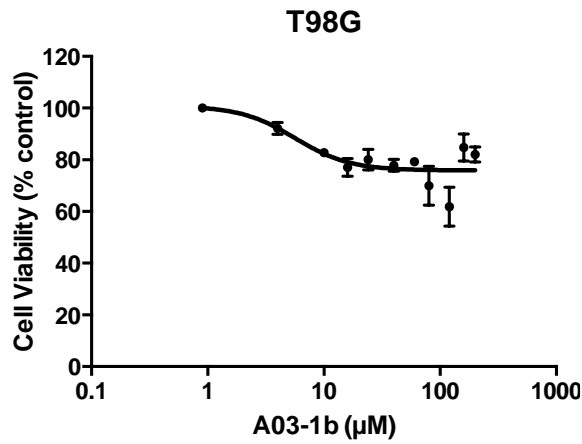
G-415



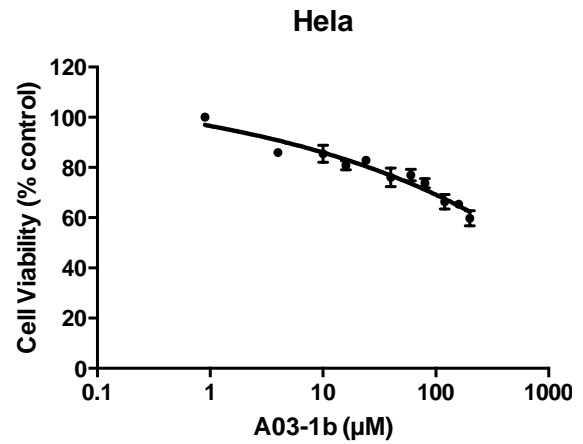
Gb-d1



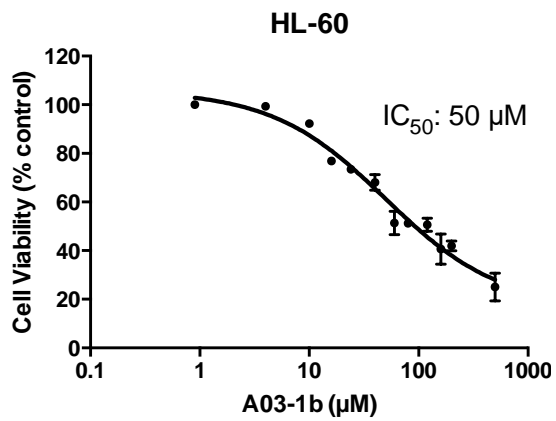
T98G



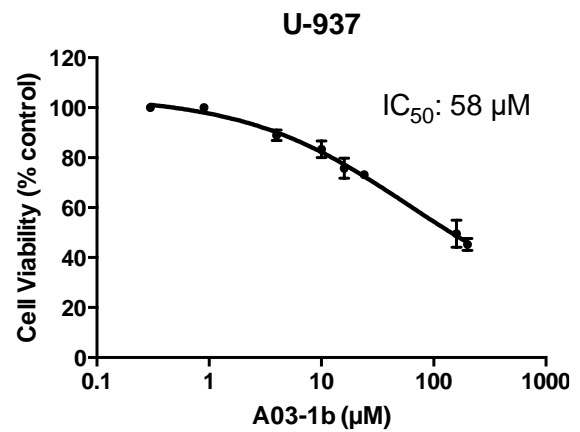
Hela



HL-60

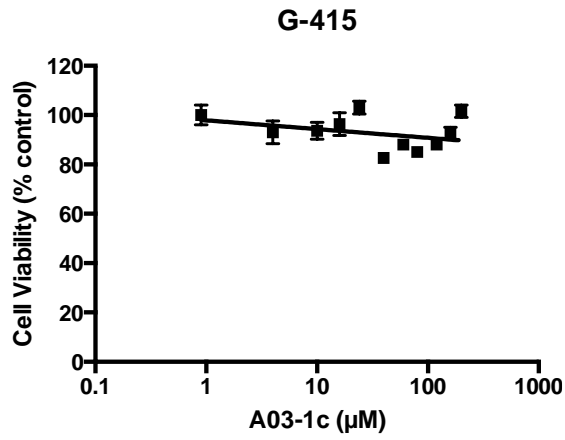


U-937

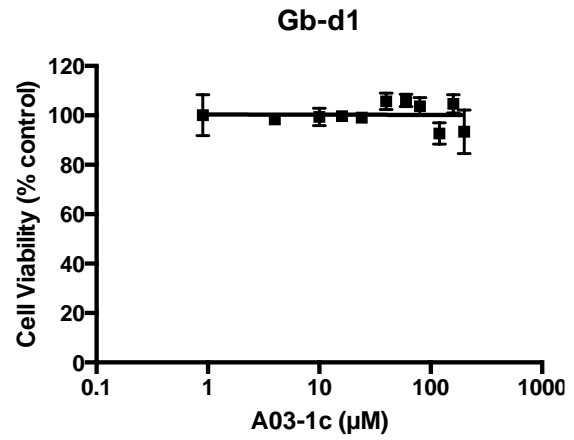


3c

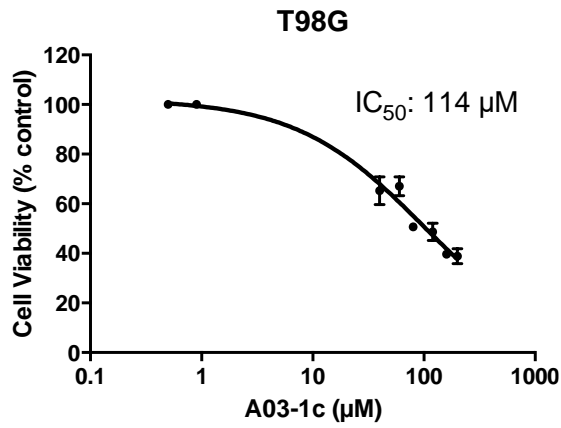
G-415



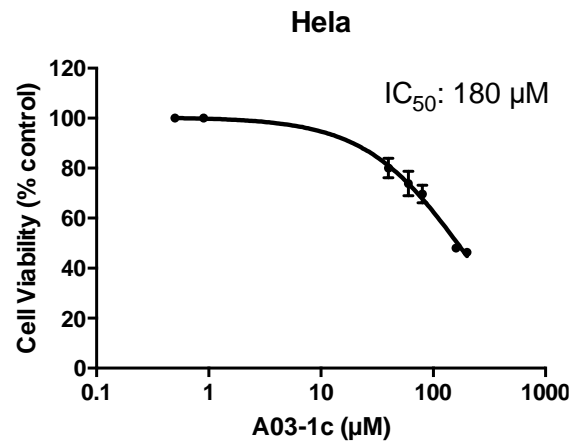
Gb-d1



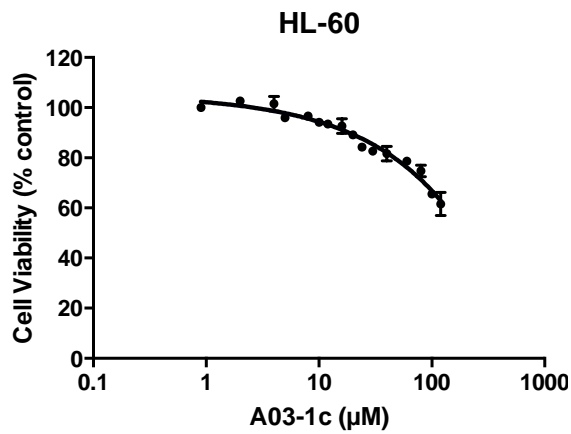
T98G



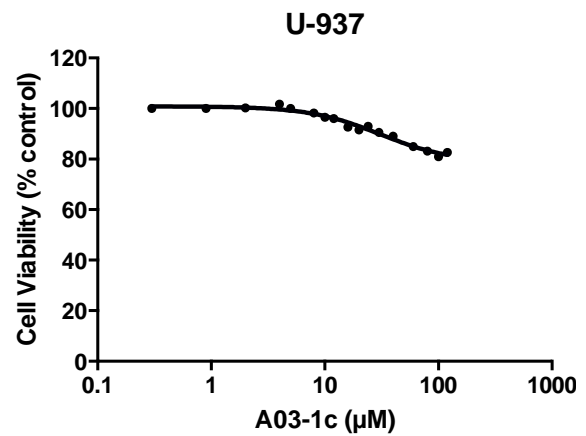
Hela



HL-60

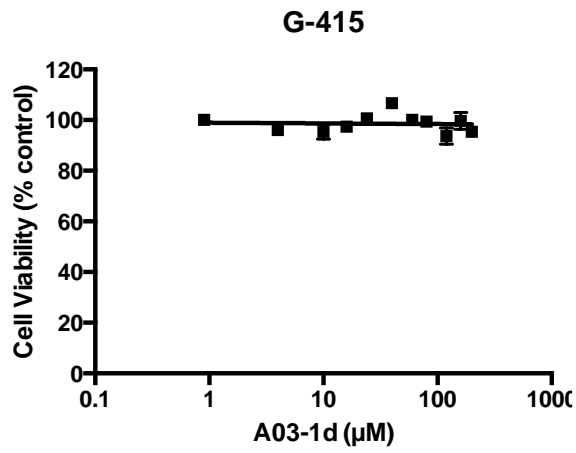


U-937

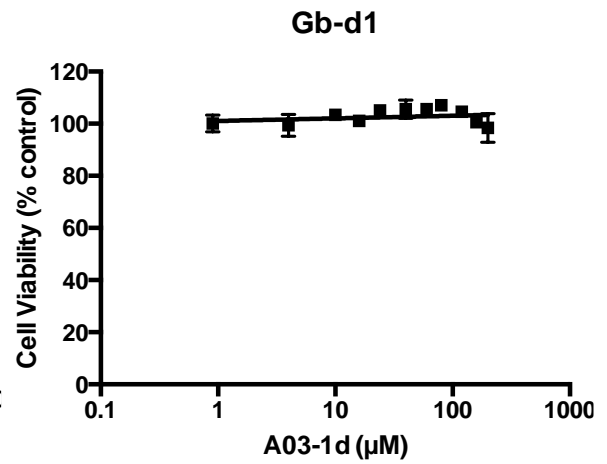


3d

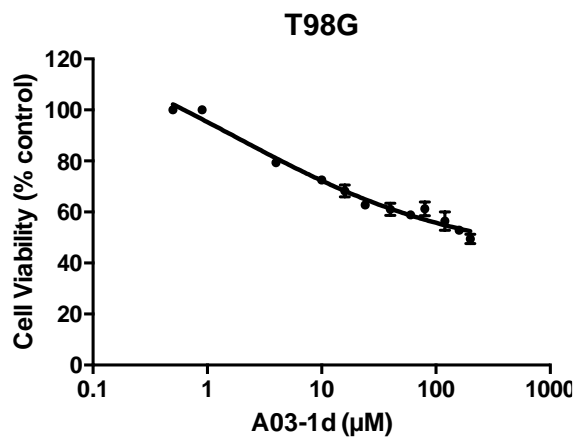
G-415



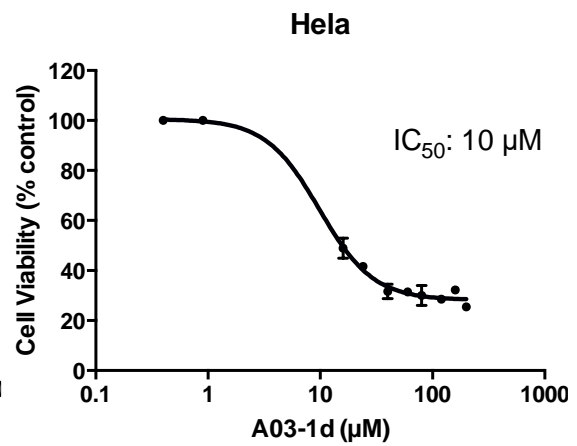
Gb-d1



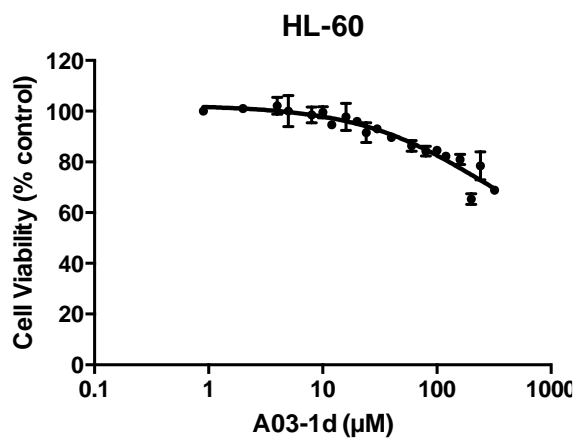
T98G



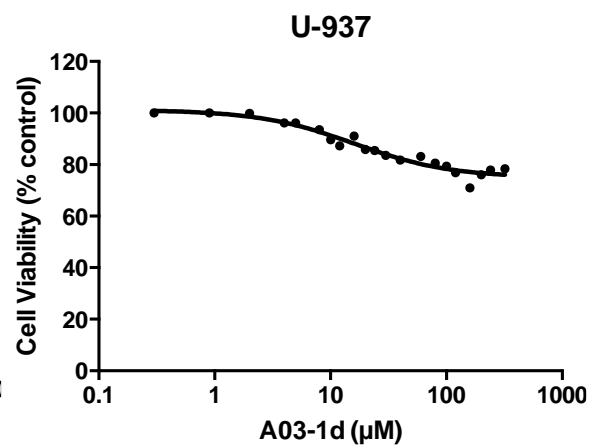
Hela



HL-60

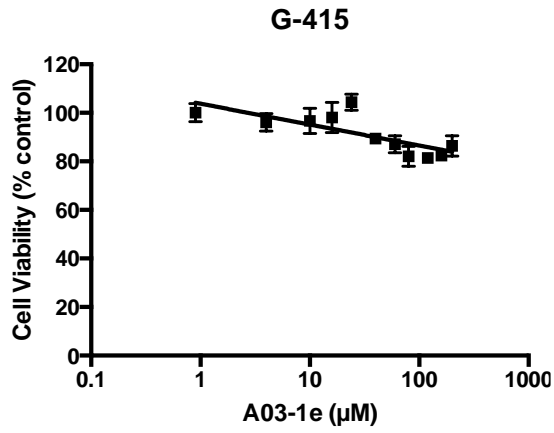


U-937

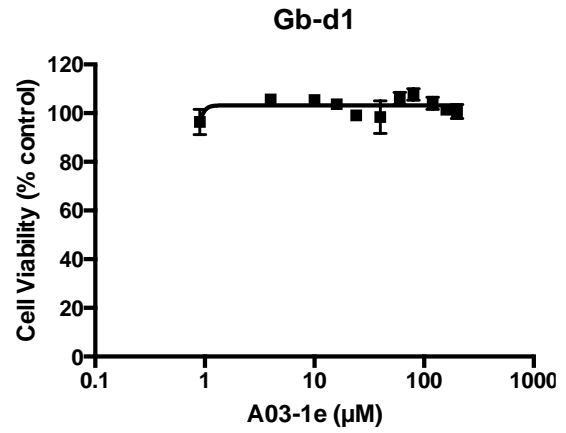


3e

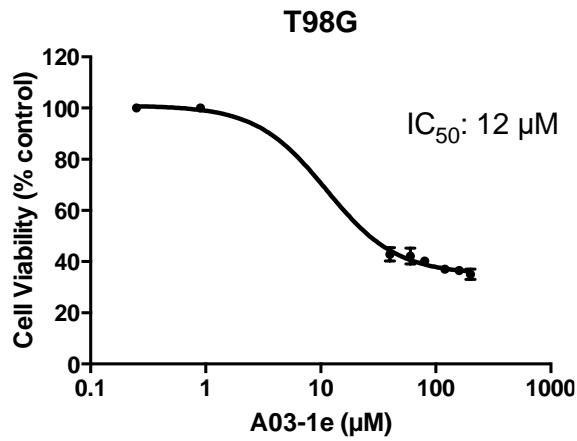
G-415



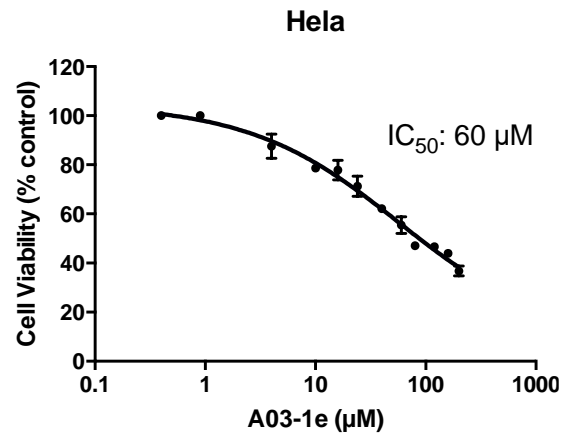
Gb-d1



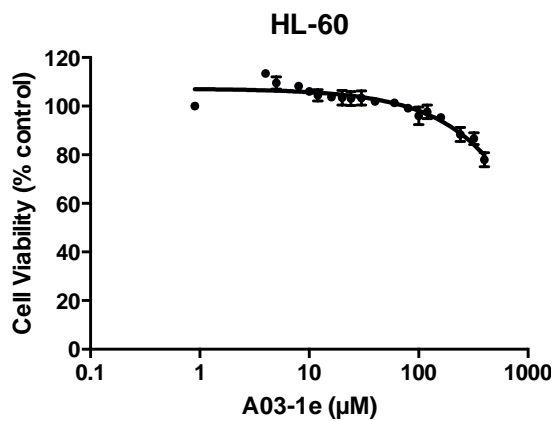
T98G



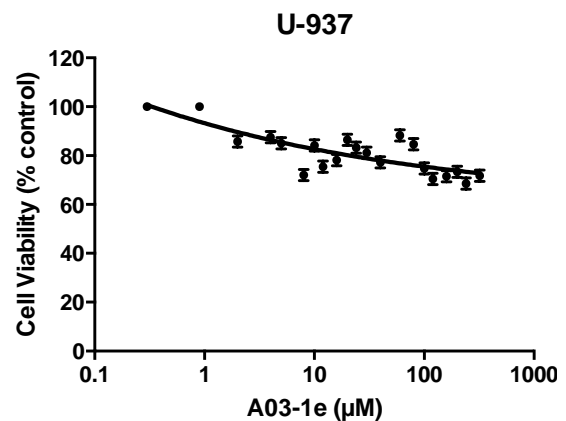
Hela



HL-60

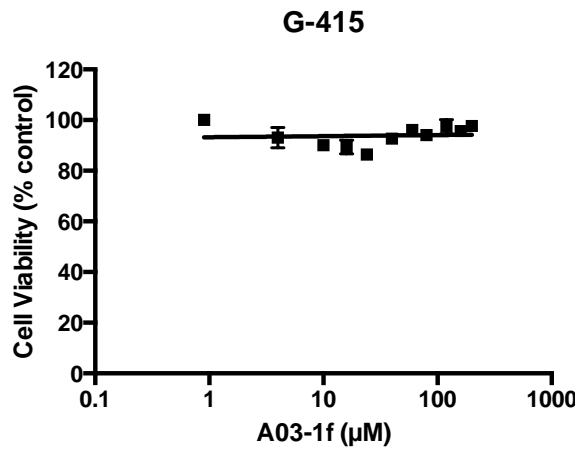


U-937

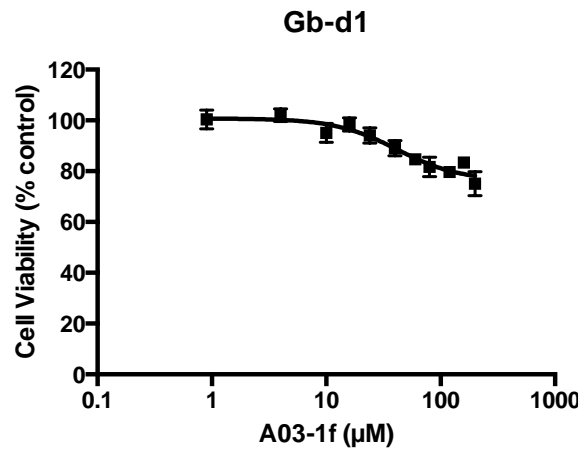


3f

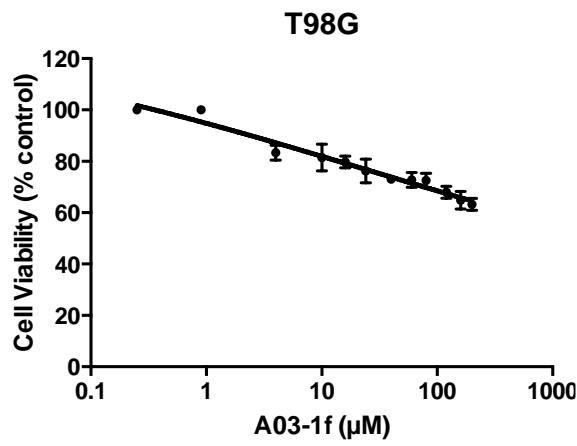
G-415



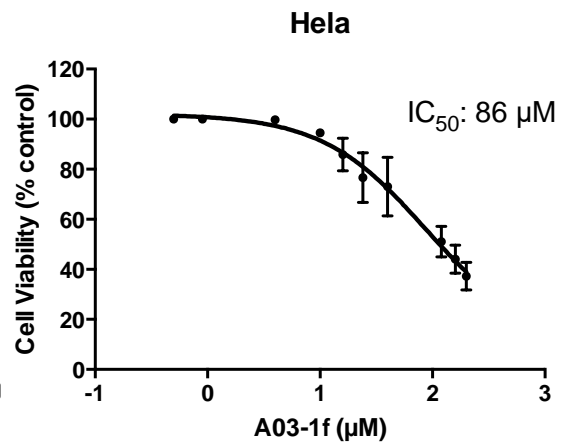
Gb-d1



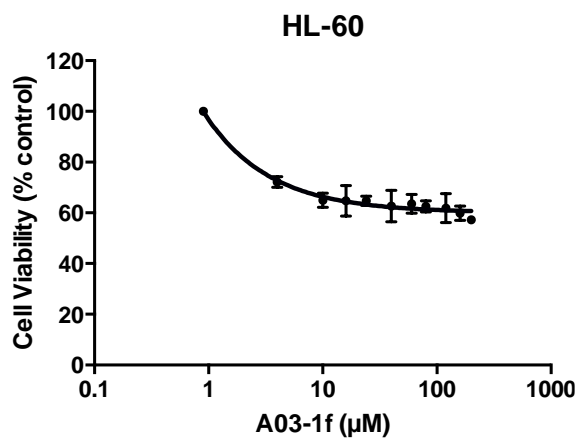
T98G



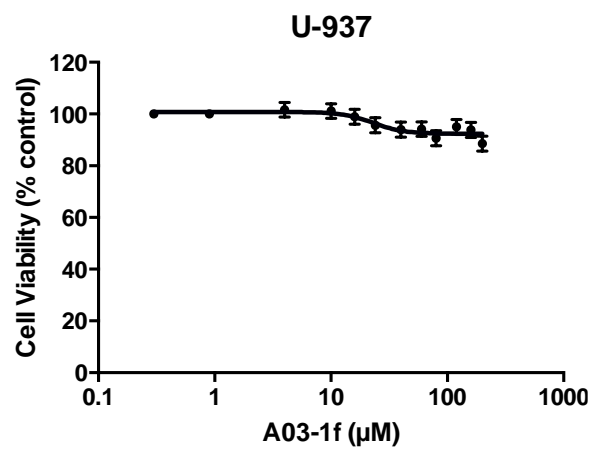
Hela



HL-60

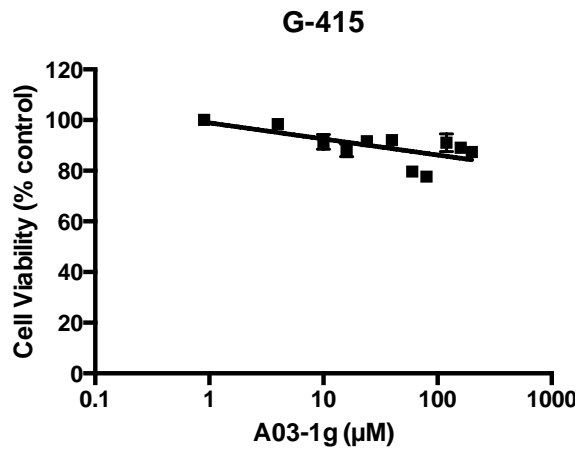


U-937

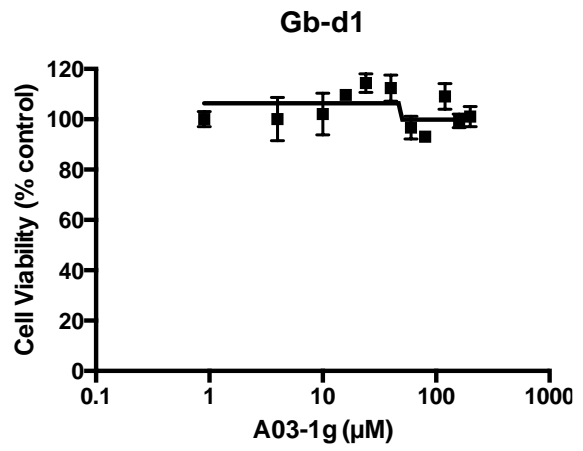


3g

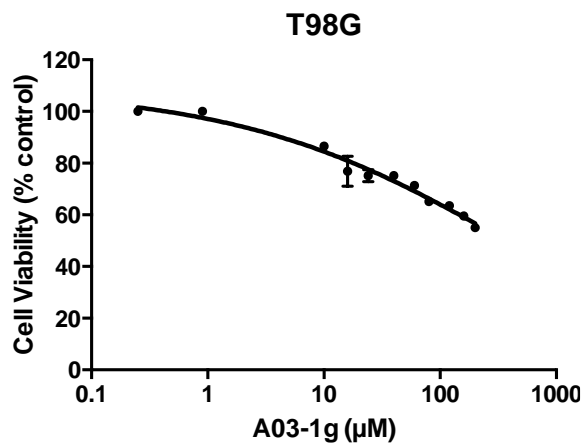
G-415



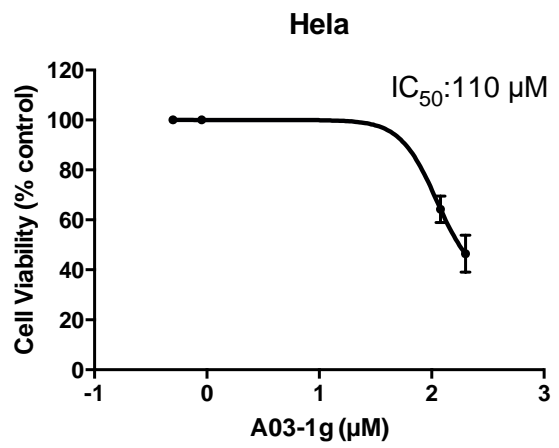
Gb-d1



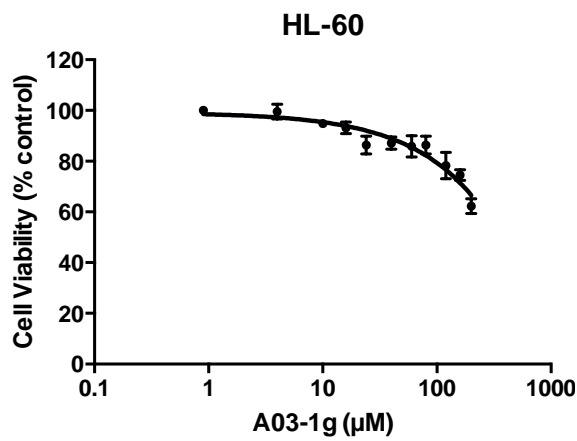
T98G



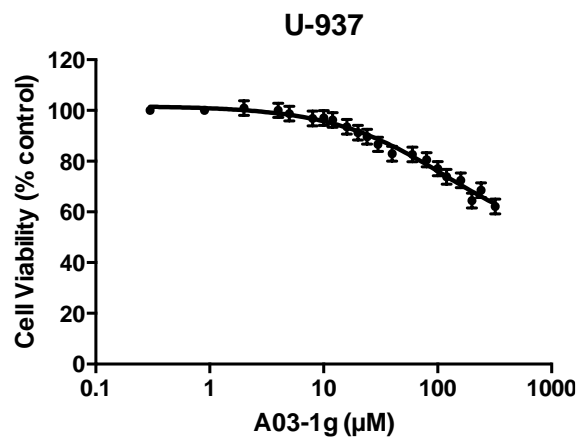
Hela



HL-60

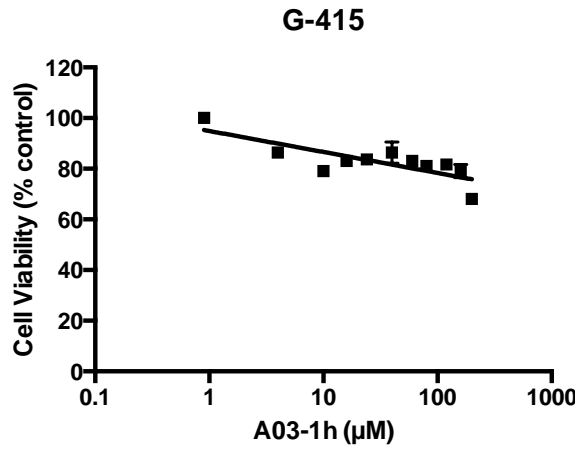


U-937

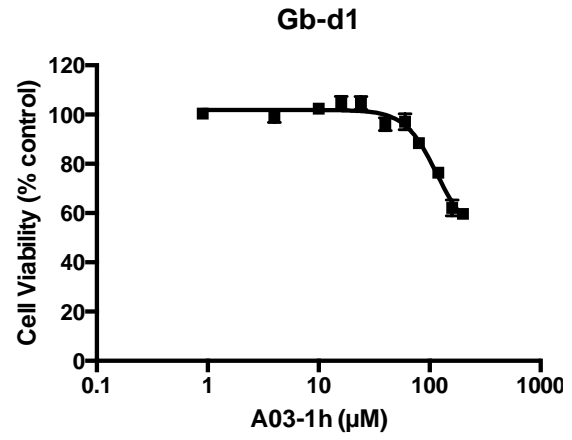


3h

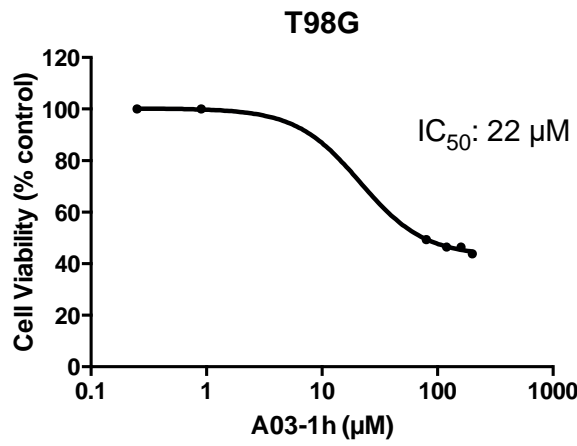
G-415



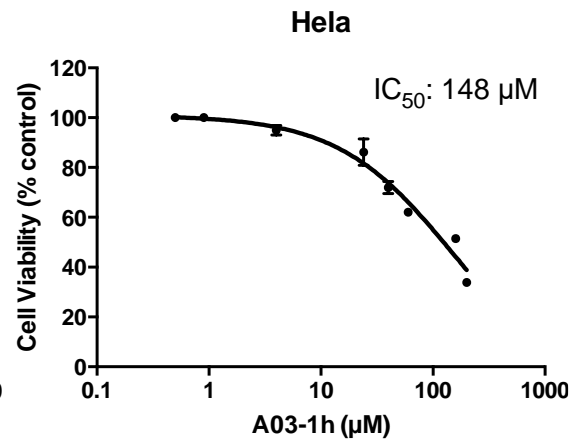
Gb-d1



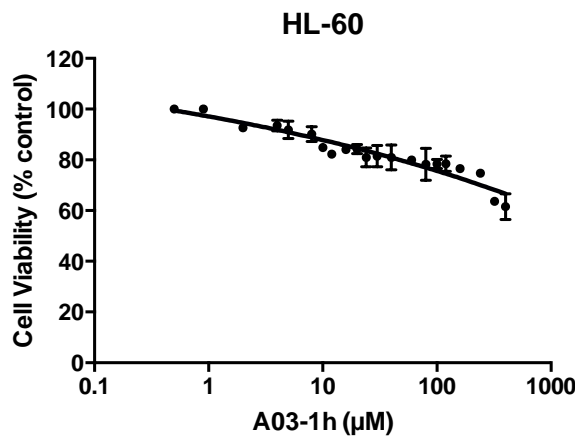
T98G



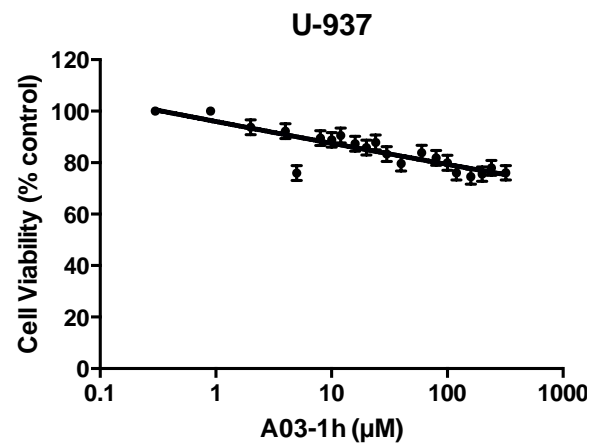
Hela



HL-60

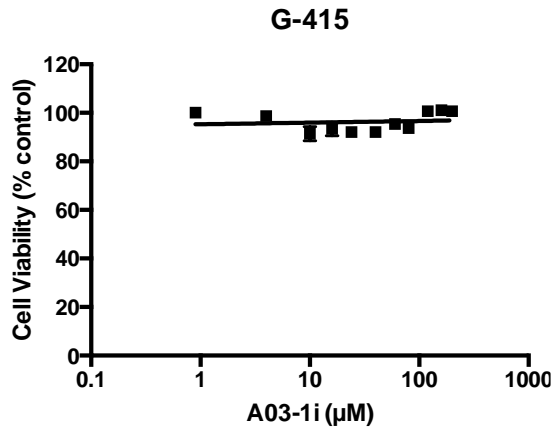


U-937

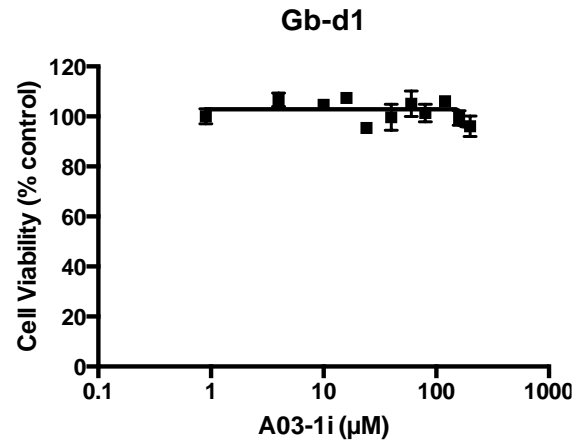


3i

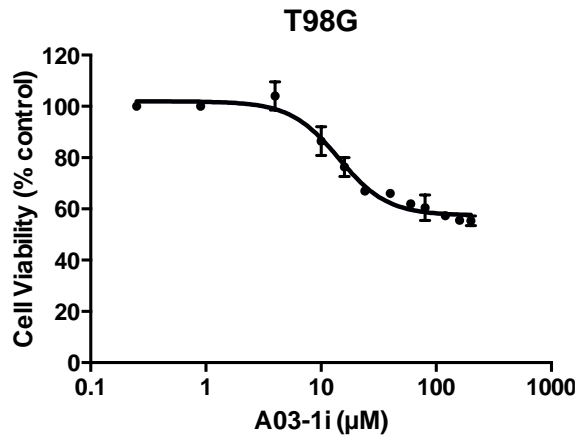
G-415



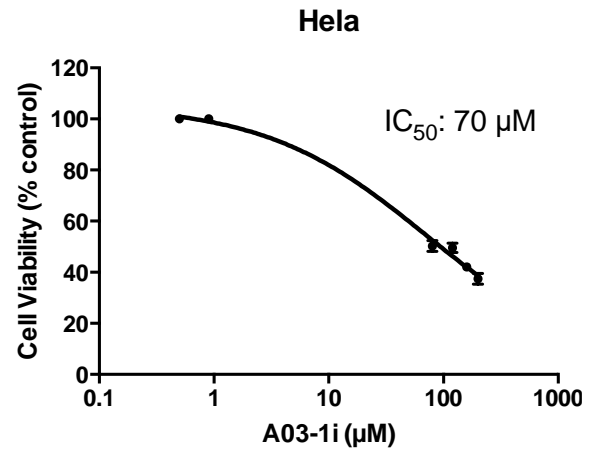
Gb-d1



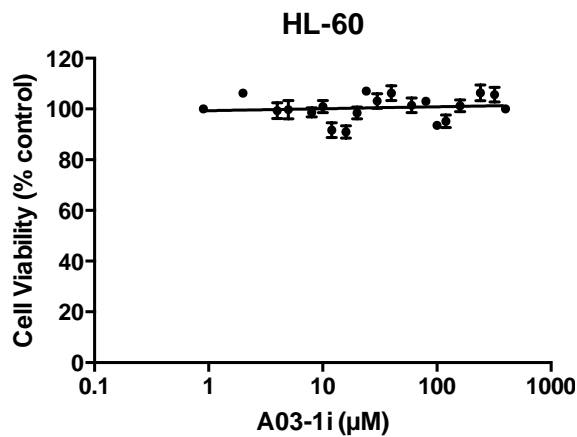
T98G



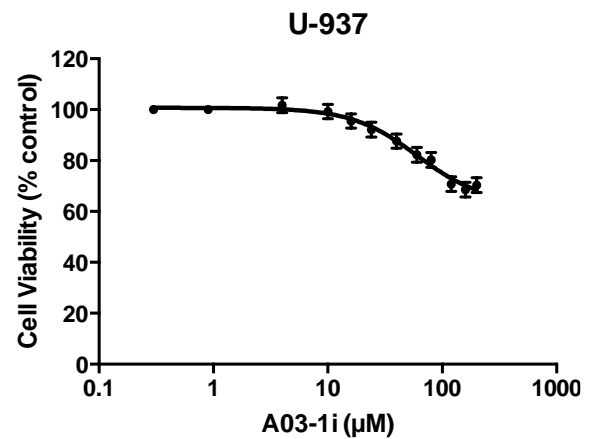
Hela



HL-60

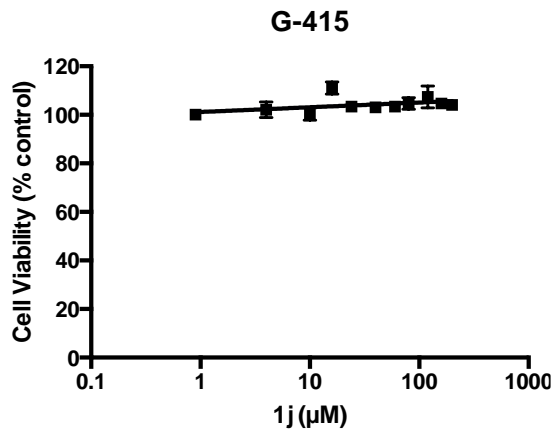


U-937

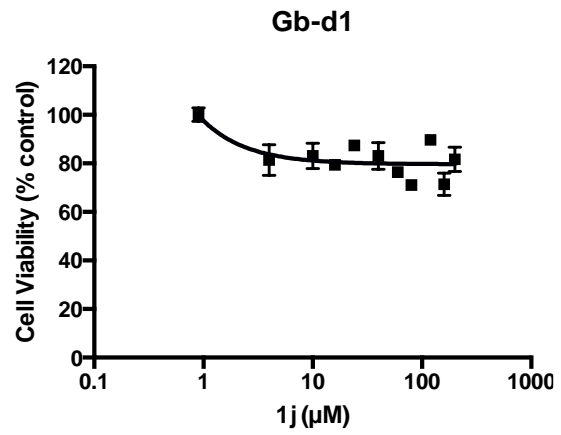


3j

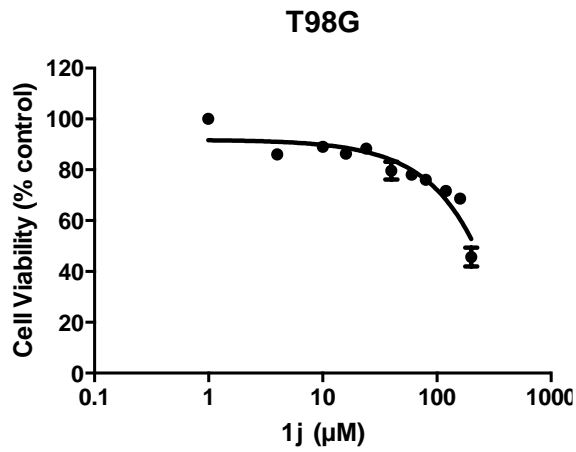
G-415



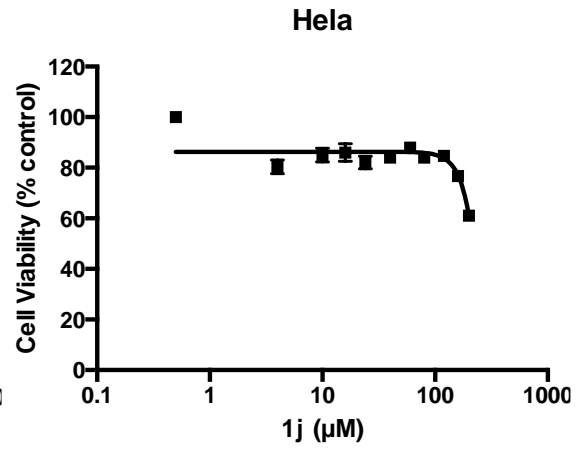
Gb-d1



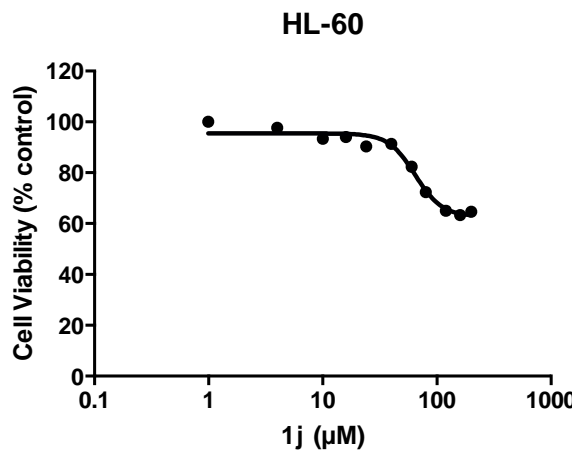
T98G



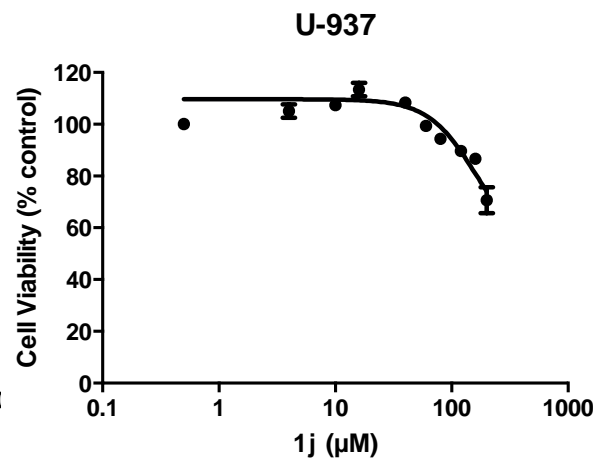
Hela



HL-60

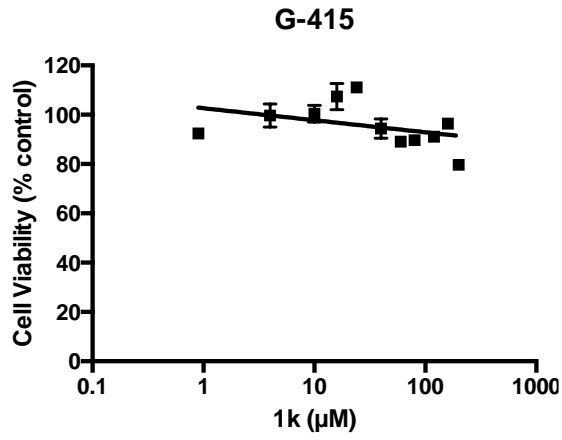


U-937

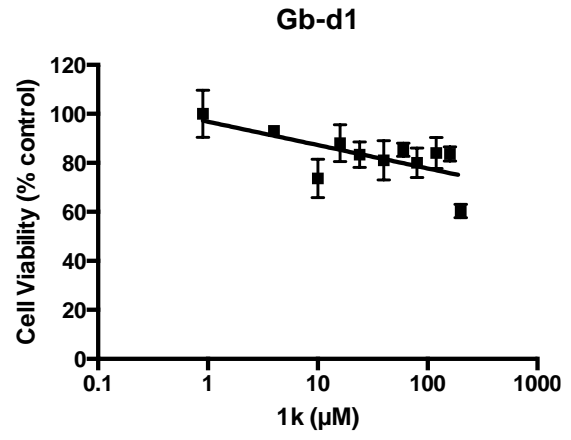


3k

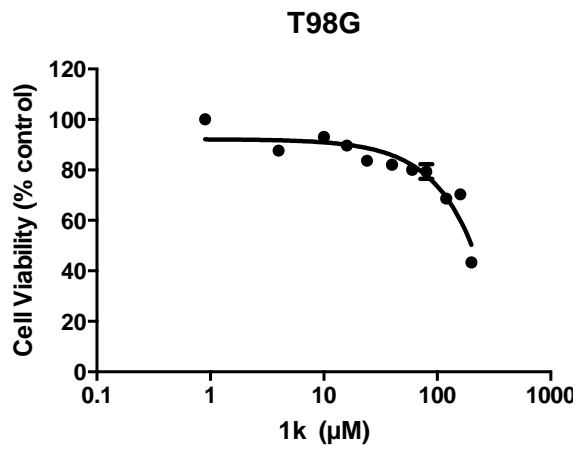
G-415



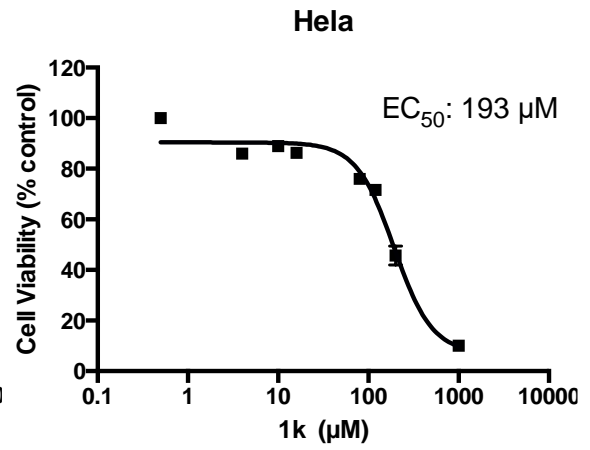
Gb-d1



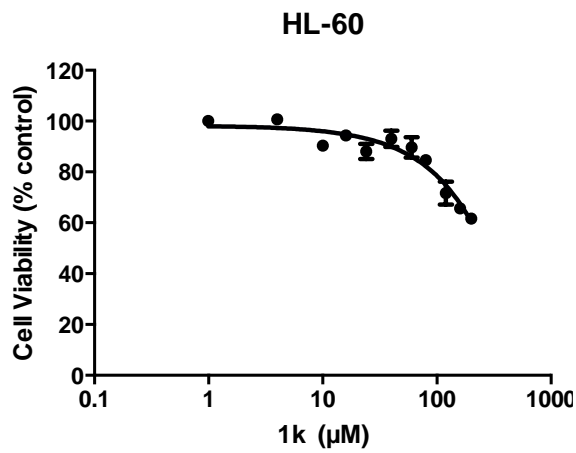
T98G



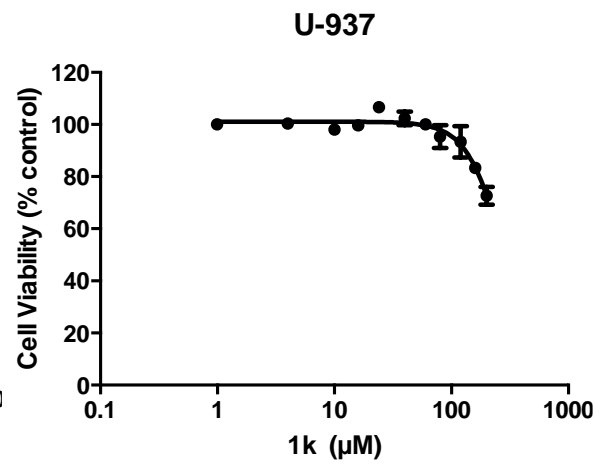
Hela



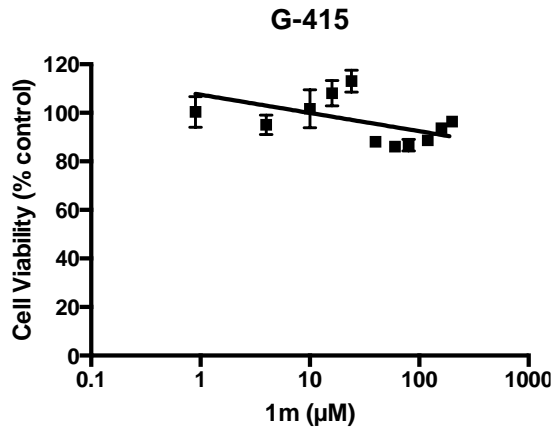
HL-60



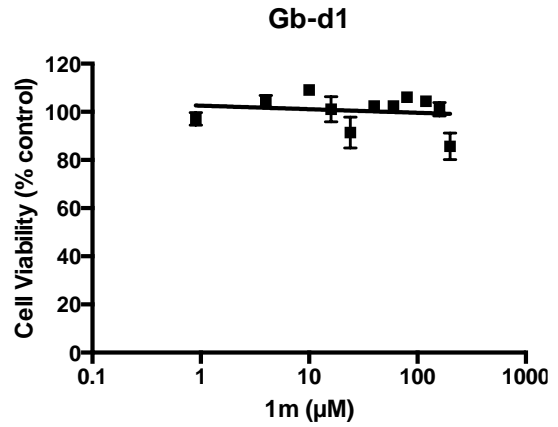
U-937



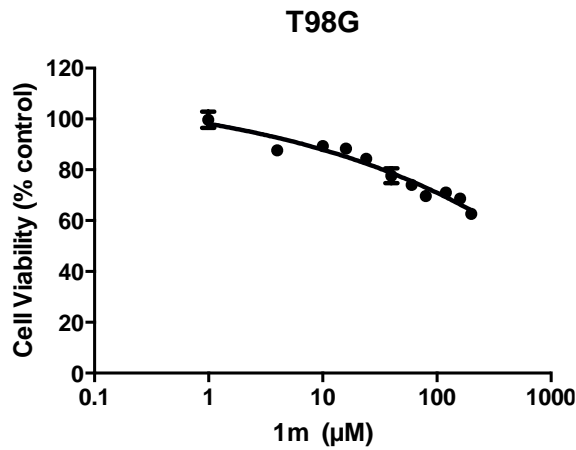
G-415



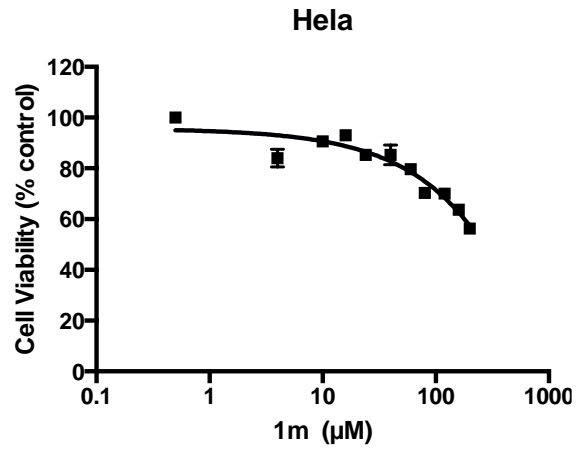
Gb-d1



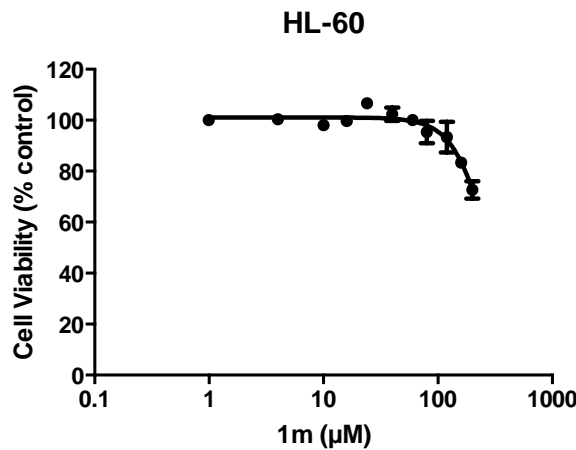
T98G



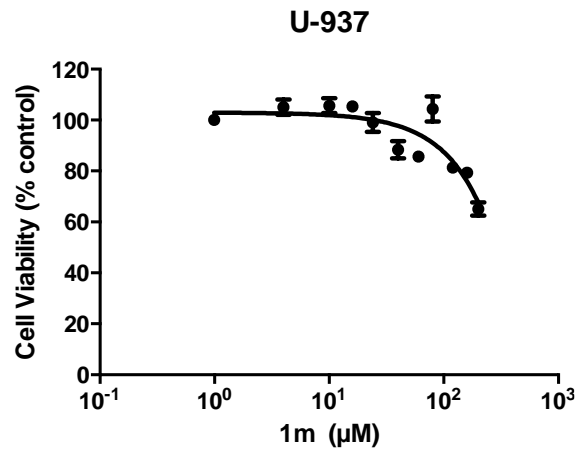
Hela



HL-60

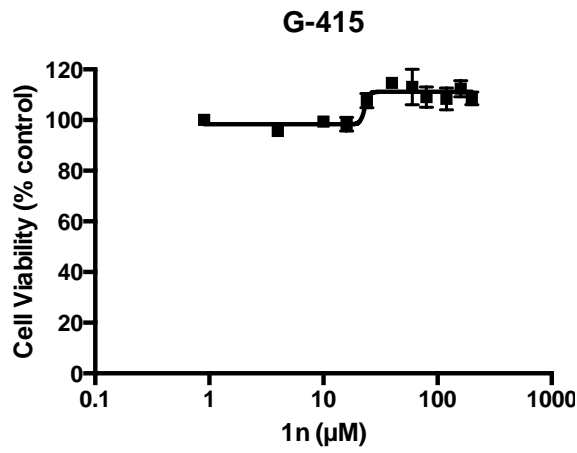


U-937

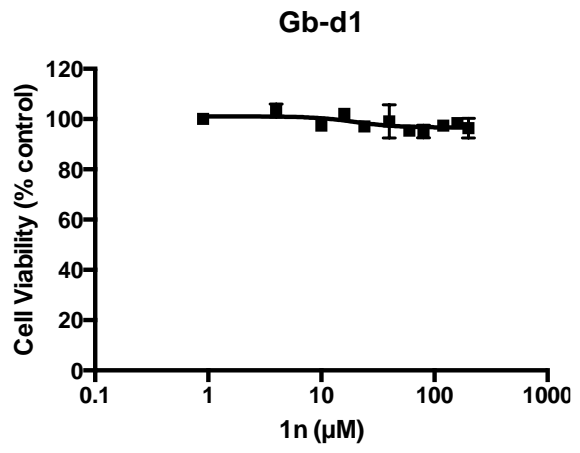


3m

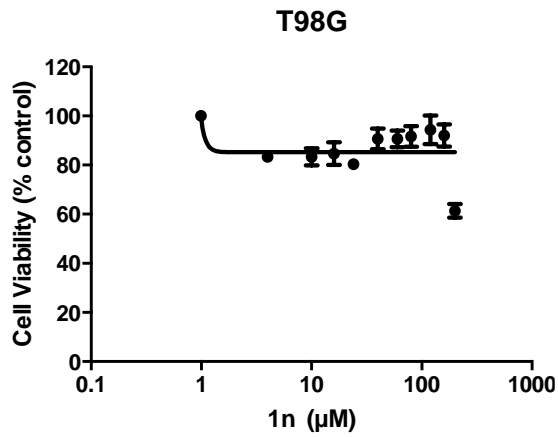
G-415



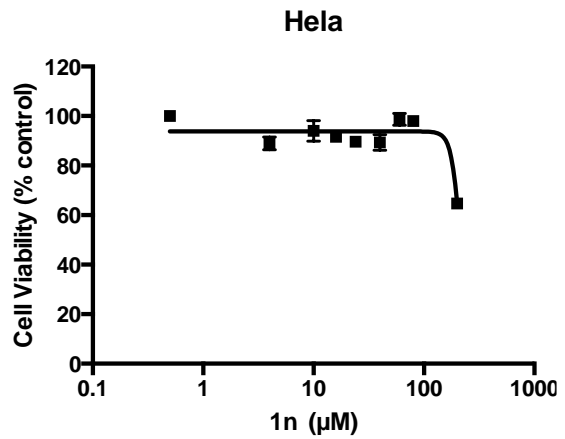
Gb-d1



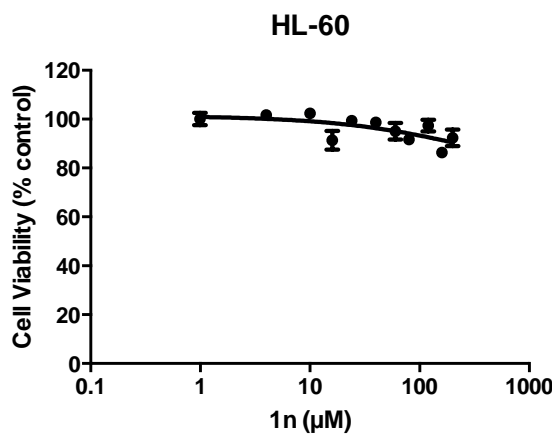
T98G



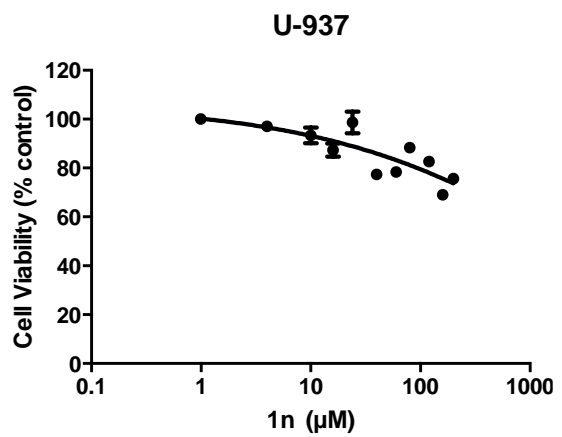
Hela



HL-60

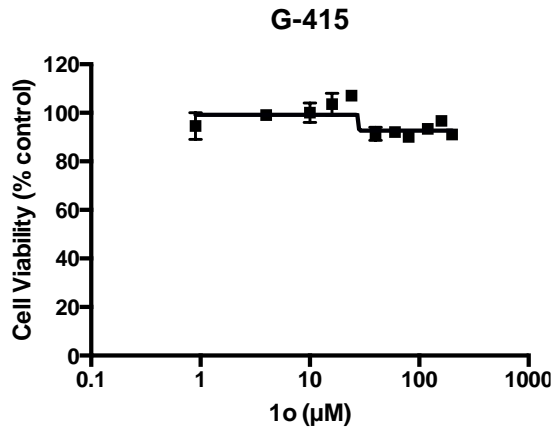


U-937

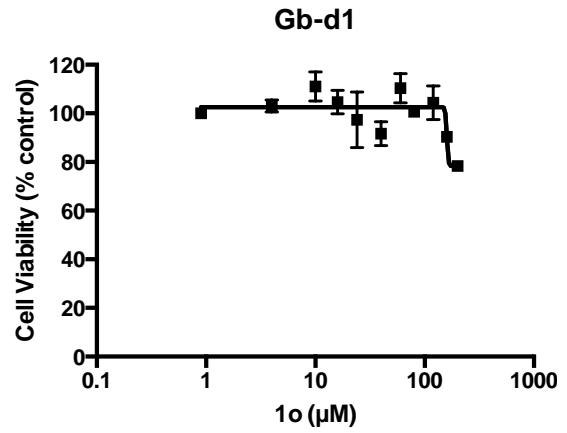


3n

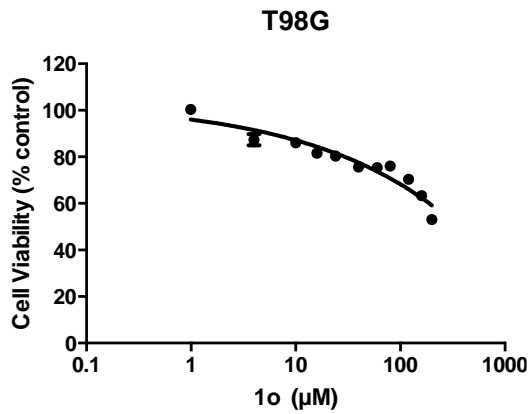
G-415



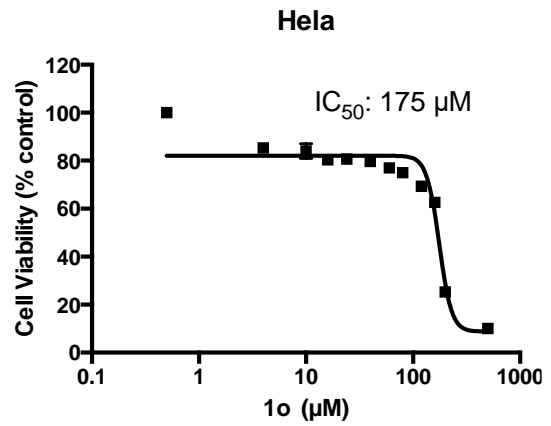
Gb-d1



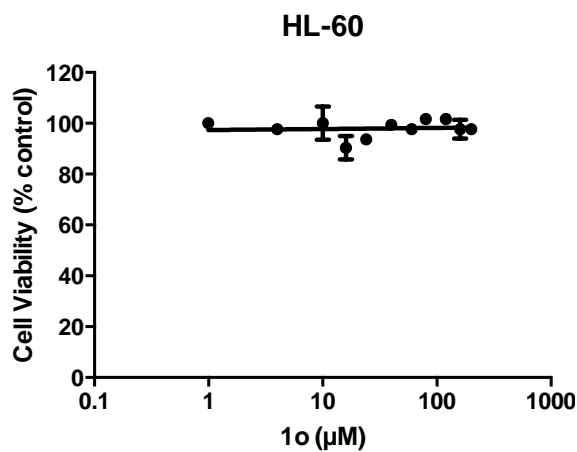
T98G



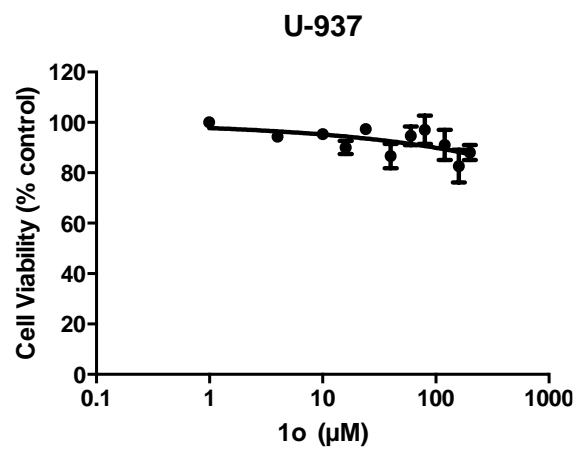
Hela



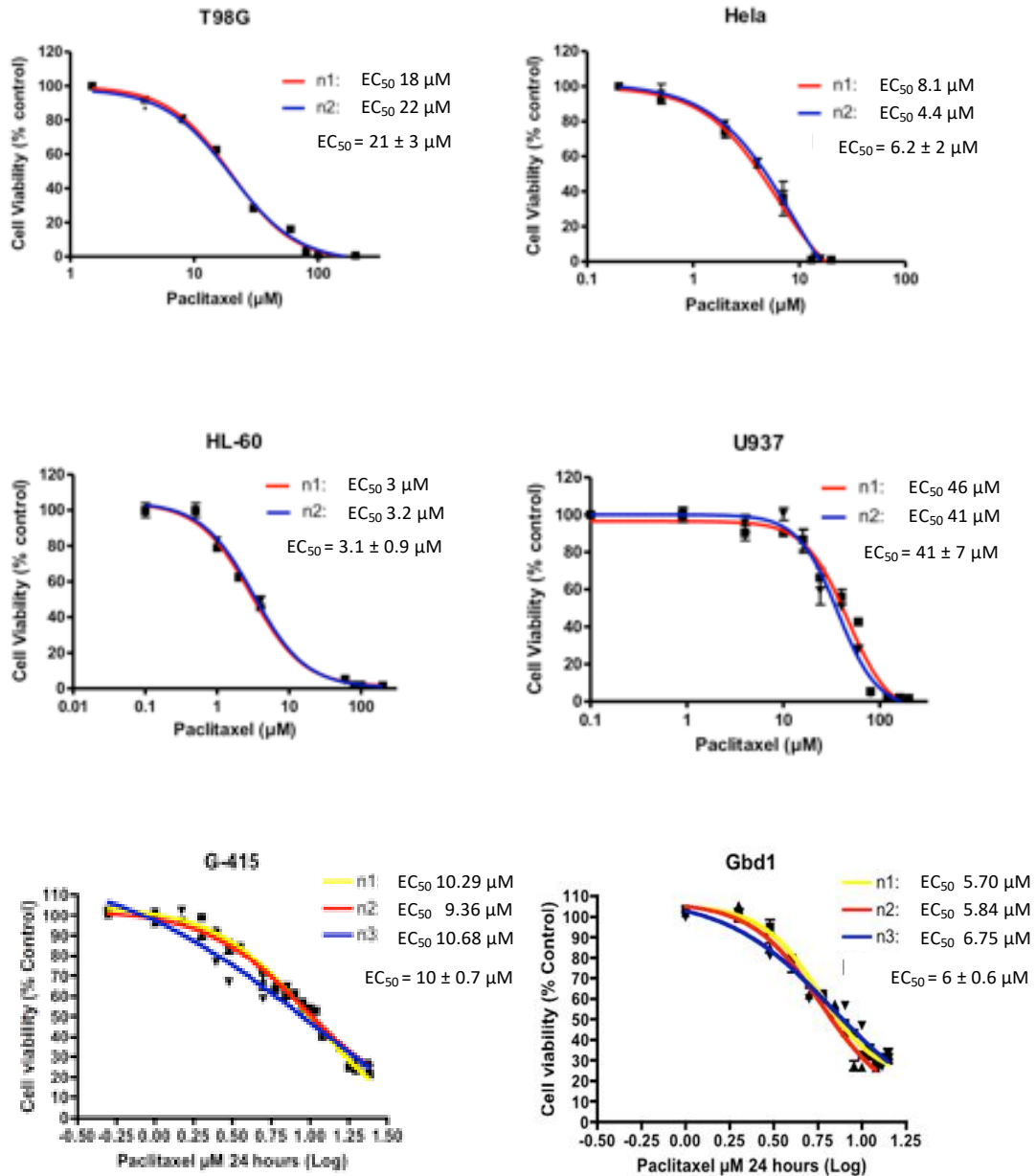
HL-60



U-937

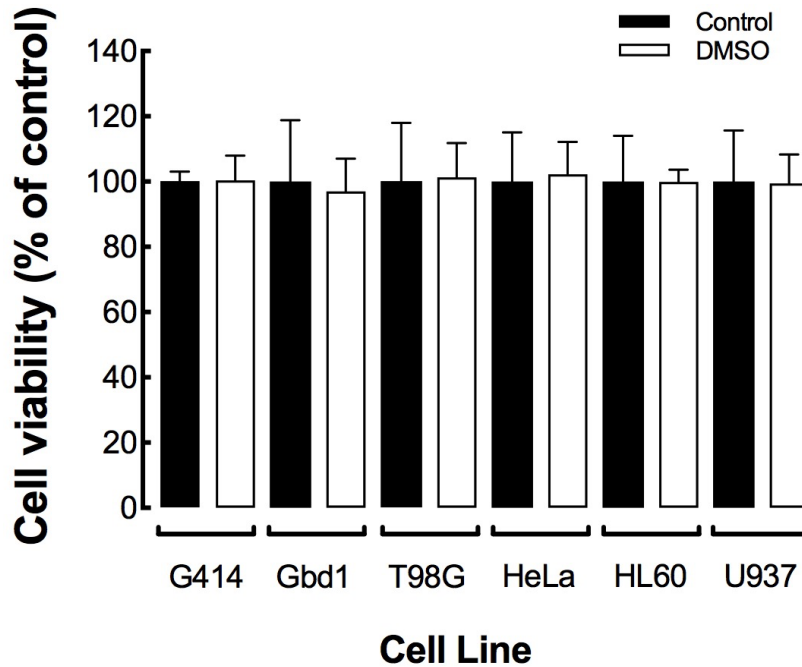


Paclitaxel (positive control)



Effect of paclitaxel on cell viability of T98G, HeLa, HL-60, U937, G-415 and Gbd1 cells. The treatments were performed by 24 h. The results are expressed as viability percentage change compared to the control sample (untreated cells). The IC_{50} values were obtained from dose-response curves by non-linear regression using *GraphPad Prism* software. Results shown for each cell line correspond to two or three independent experiments each in triplicate, and the IC_{50} values are presented as mean \pm SD.

DMSO (negative control)



Effect of DMSO on viability of cancer cell lines. Cells were seeded in a 96-well microtiter plate at a density of 5×10^5 /mL and incubated for 24 hours. Next, the cells were treated with culture medium (Control) or culture medium plus 1% DMSO and incubated by 24 h. After incubation, cells were subjected to the MTT assay for viability, similarly to that previously described. Sixfold assays were used for each of the cell lines ($n=6$). From the absorbance readings of the MTT assay, the mean and standard deviation (SD) were obtained. Finally, the data obtained were normalized with the means of their respective controls. To determine statistical differences between the control and the respective treatment with DMSO, a t-student test was applied using a confidence level with $p < 0.05$. The figure shows mean \pm SD. No statistically significant differences were obtained.

3. Pathak's structures for 3D-QSAR study

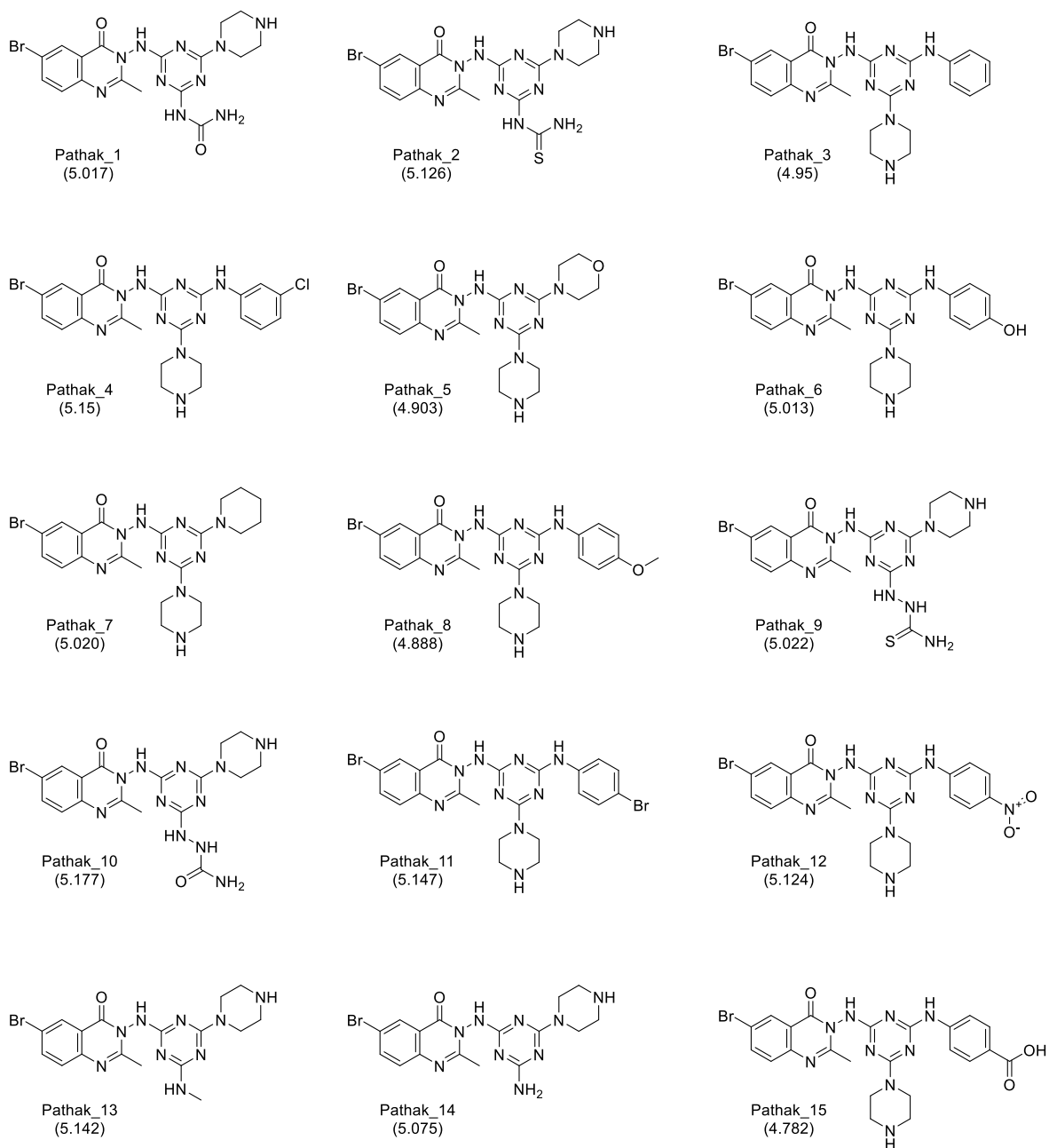


Figure S1. Pathak's structures (15 molecules) and experimental pIC50 in parentheses.

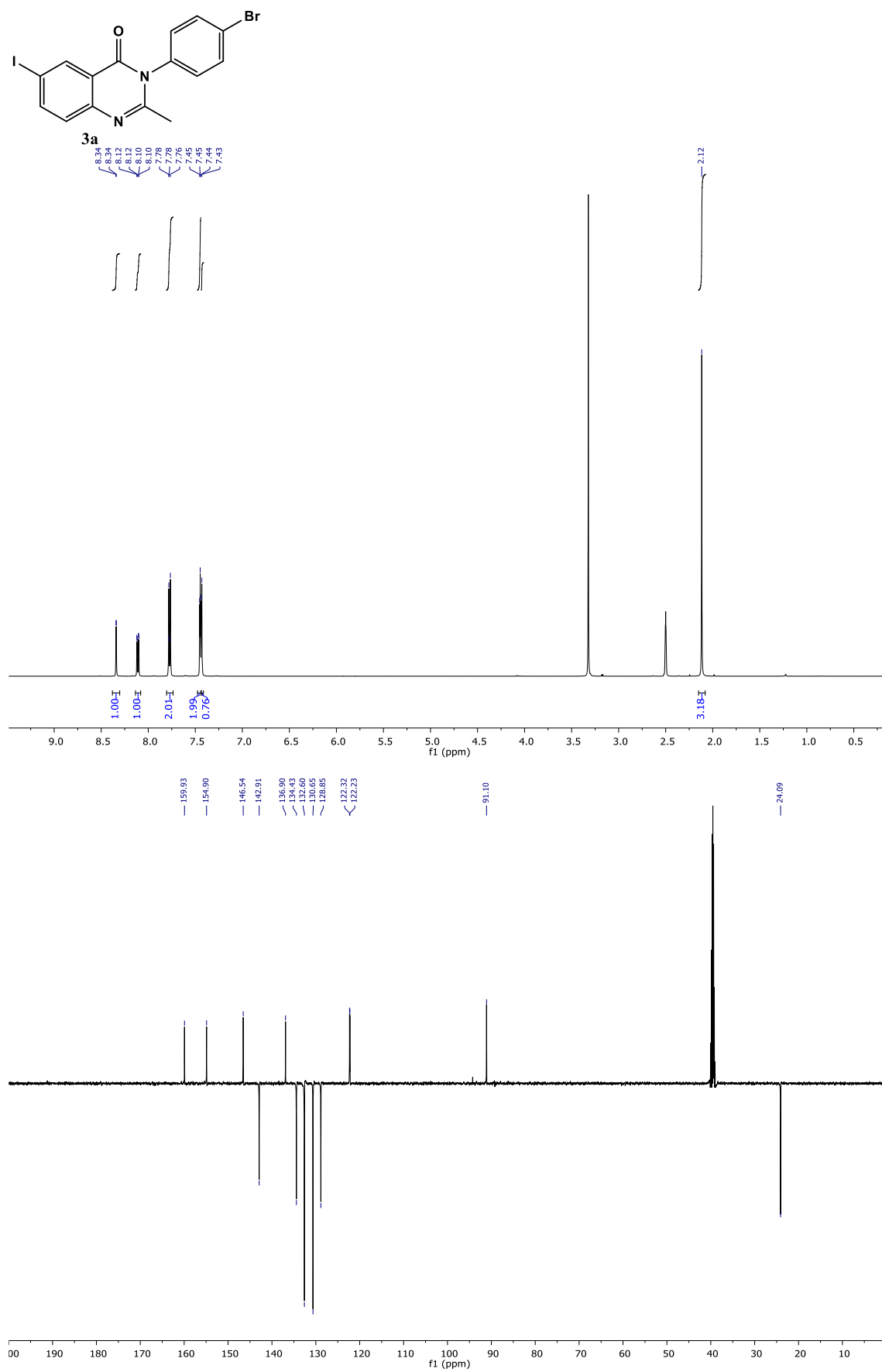
4. Principal spectroscopy data

Principal spectroscopy data of the 6-iodo-2-methylquinazolin-4(3*H*)-one derivatives.^[a]

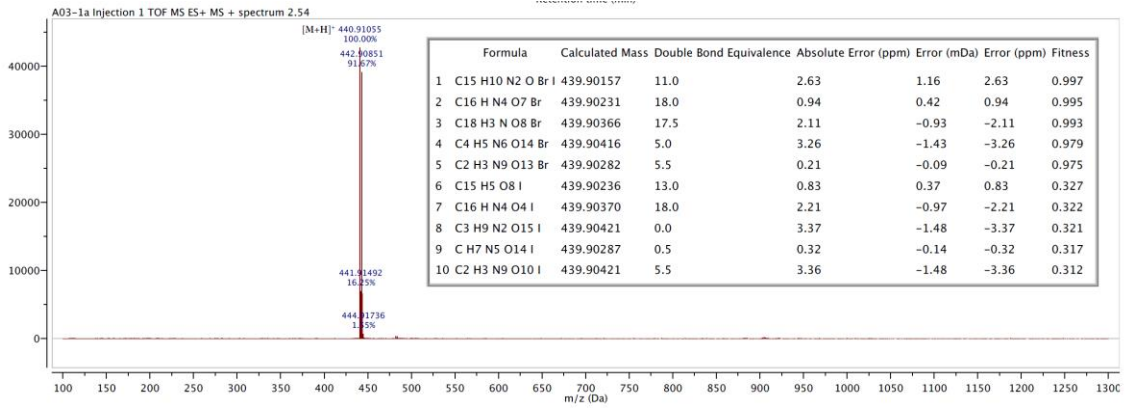
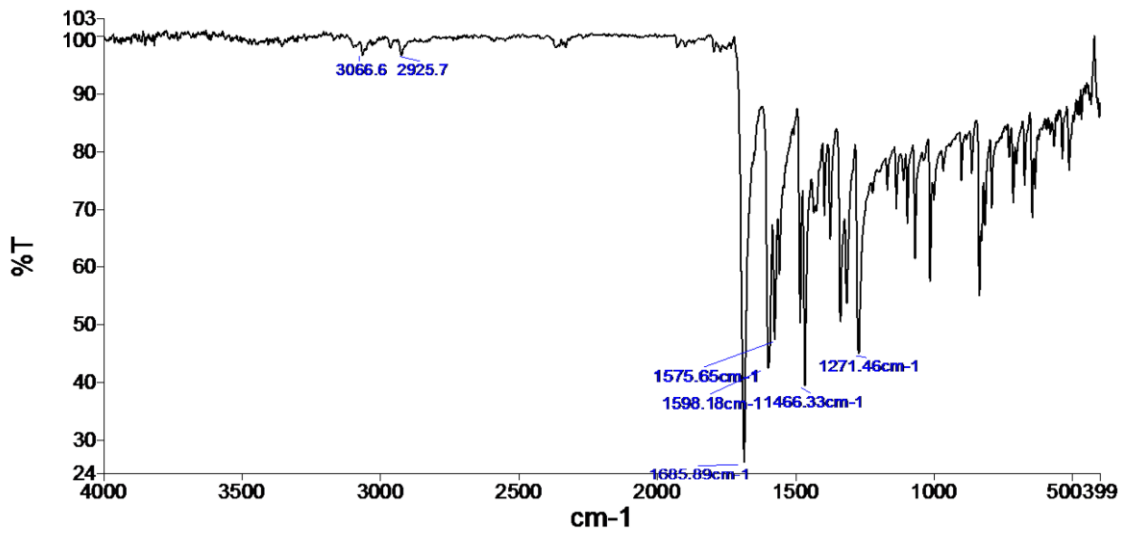
Comp.	IR (cm ⁻¹)		¹ H NMR (ppm)		¹³ C NMR (ppm)	
	C=O	C=N	Me (H ₁₂)	C=O (C ₄)	C ₂	C-I (C ₆)
3a	1685	1598	2.12	159.9	154.9	91.1
3b	1676	1604	2.12	159.9	154.9	91.1
3c	1672	1610	2.12	160.2	159.3	90.9
3d	1671	1603	2.15	159.9	154.7	91.2
3e	1675	1609	2.14	160.2	155.5	91.0
3f	1673	1608	2.16	160.1	155.9	90.9
3g	1679	1602	2.13	159.9	154.3	91.3
3h	1671	1603	2.14	160.0	157.3	91.1
3i	1672	1600	2.49	158.9	158.5	91.3
3j	1673	1616	2.13	160.1	154.6	91.2
3k	1667	1596	2.12	160.0	155.5	90.9
3l	1656	1616	2.45	159.9	155.9	91.0
3m	1652	1613	2.11	160.3	157.7	91.0
3n	1681	1603	2.23	159.6	154.3	91.8

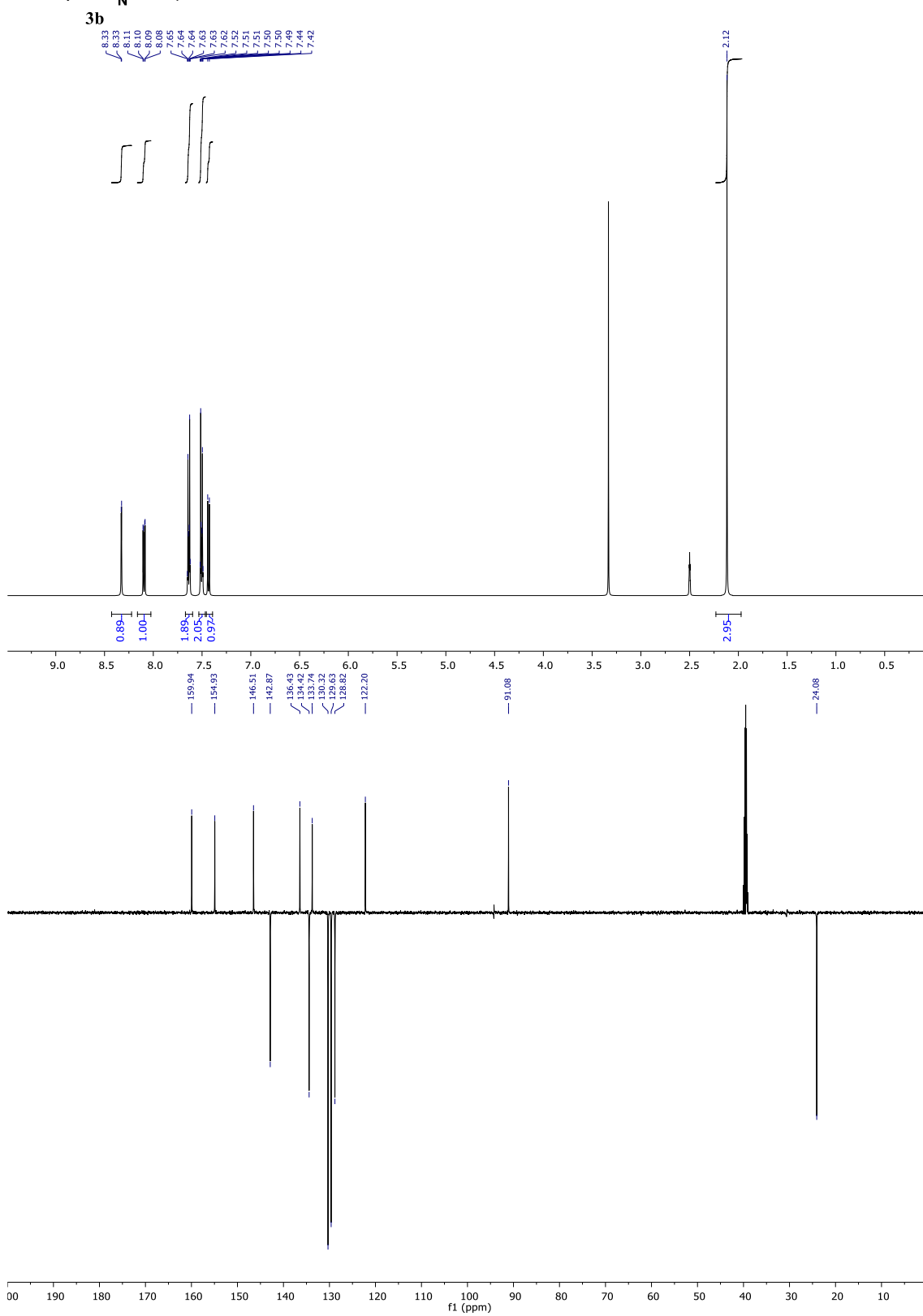
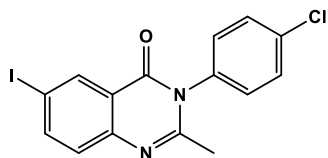
[a] NMR carried out in DMSO-*d*₆

5. ^1H NMR, ^{13}C NMR-APT, FT-IR and HRESIMS spectra of compounds

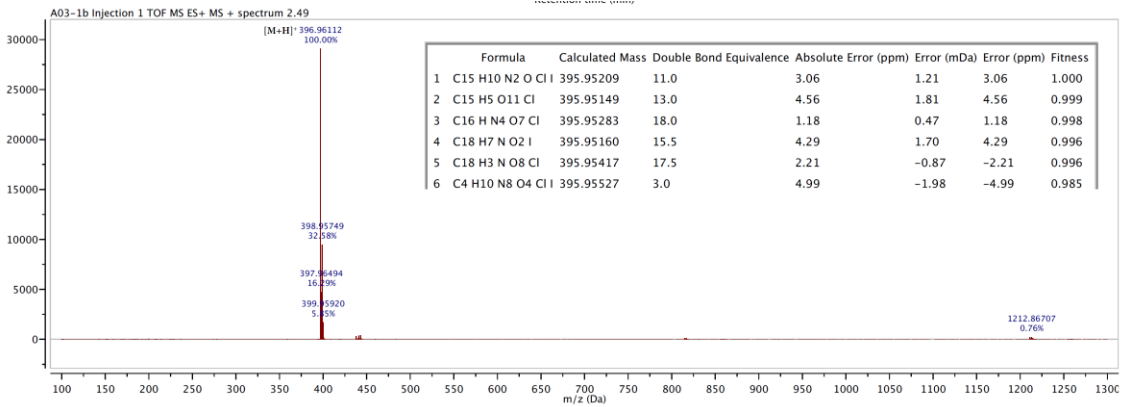
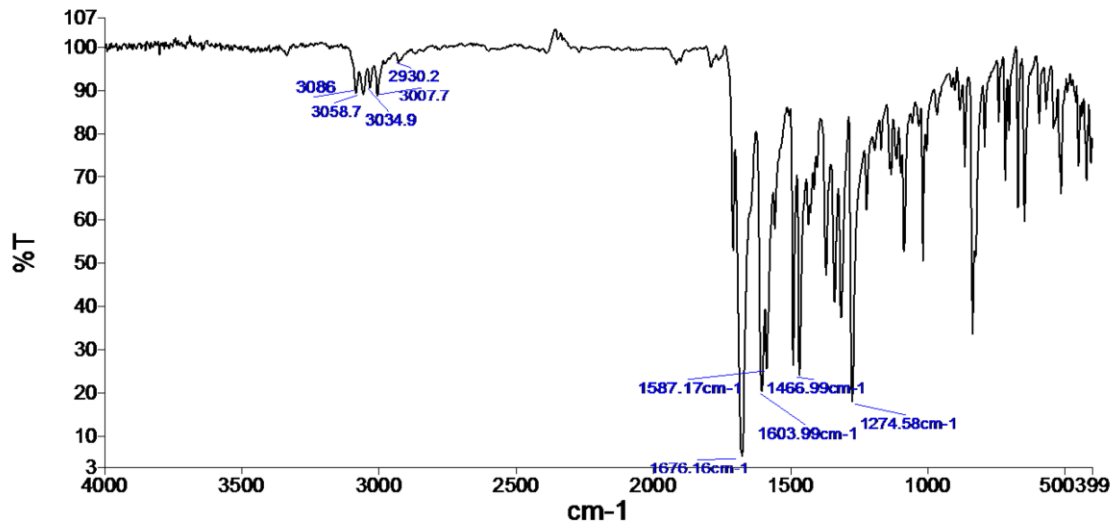


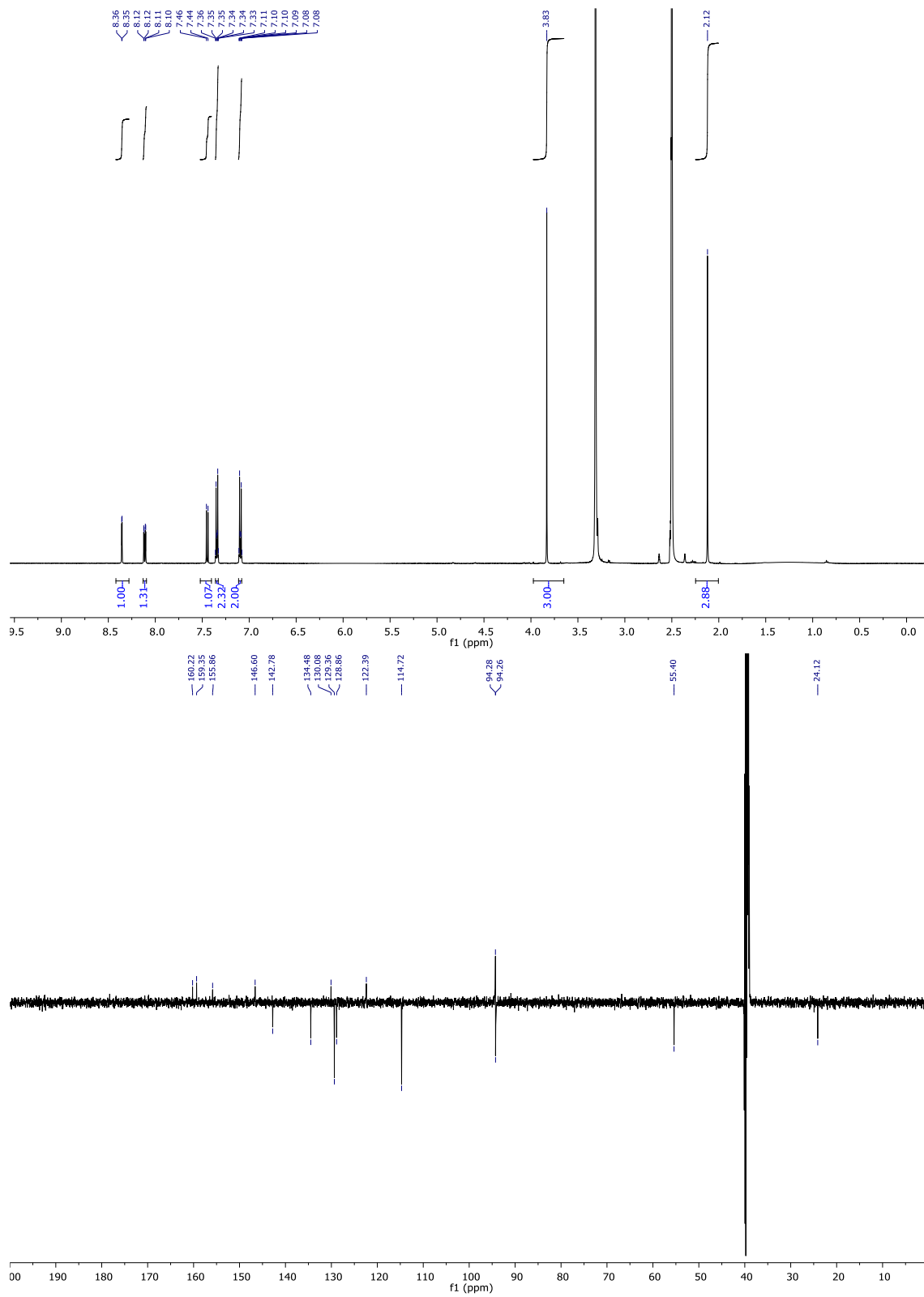
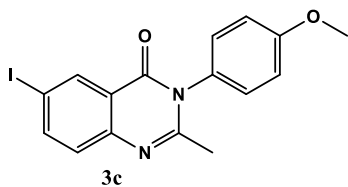
Spectrum



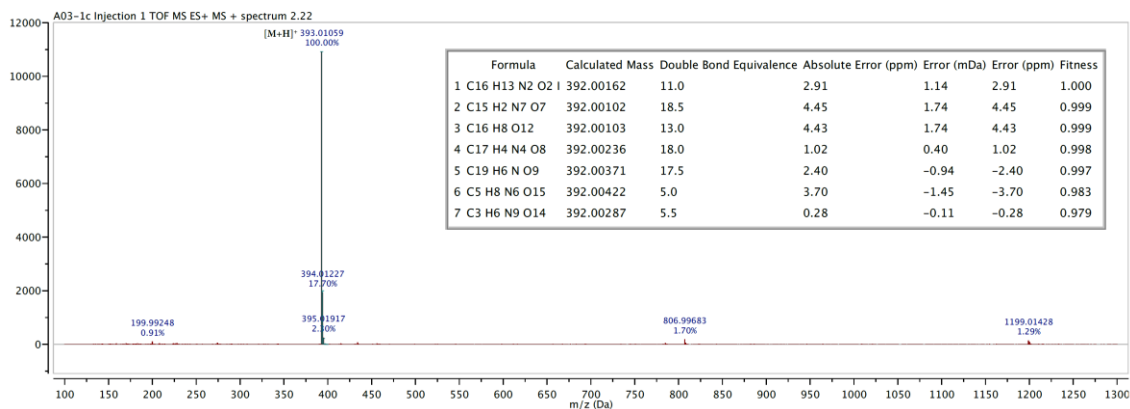
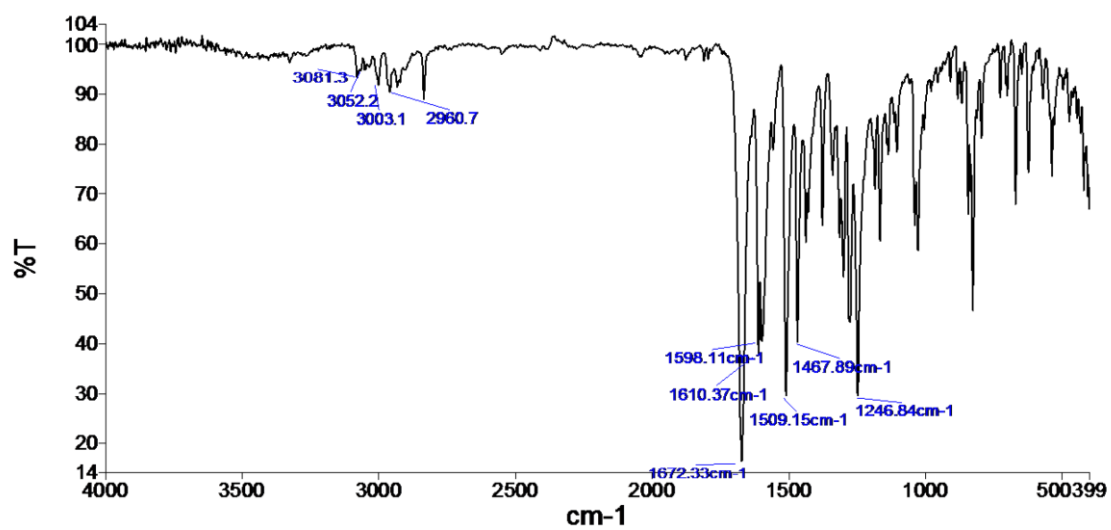


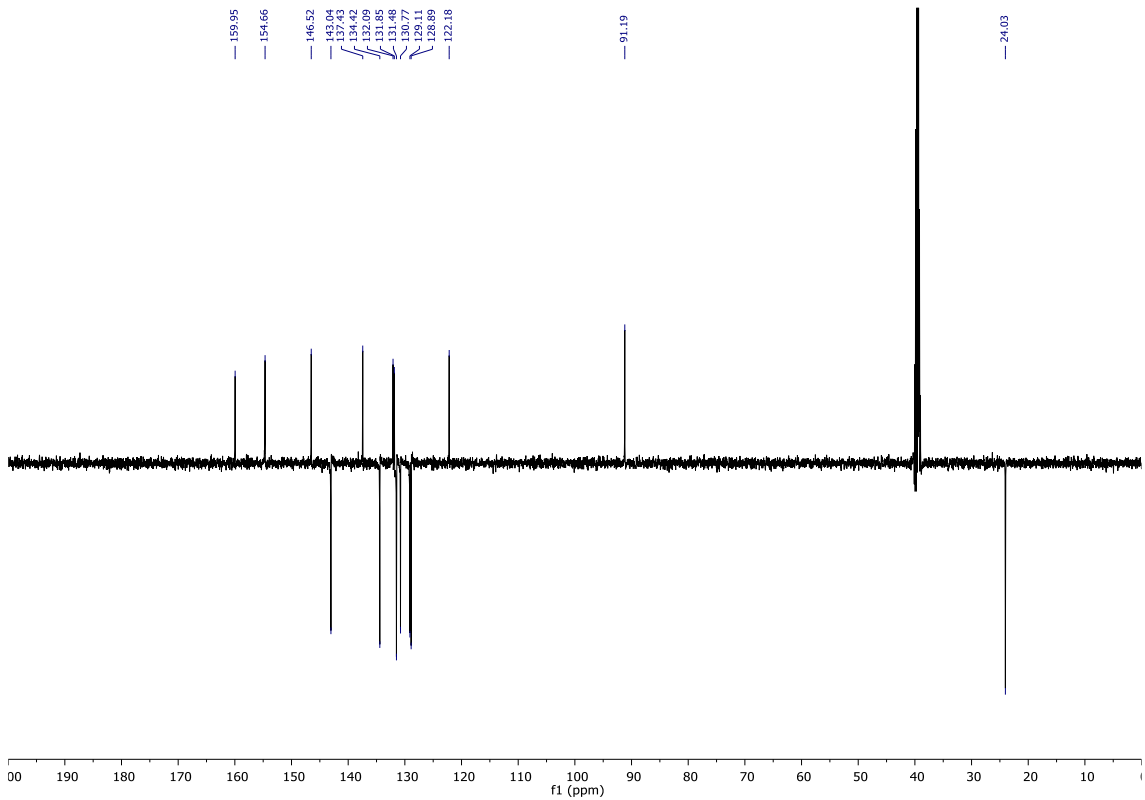
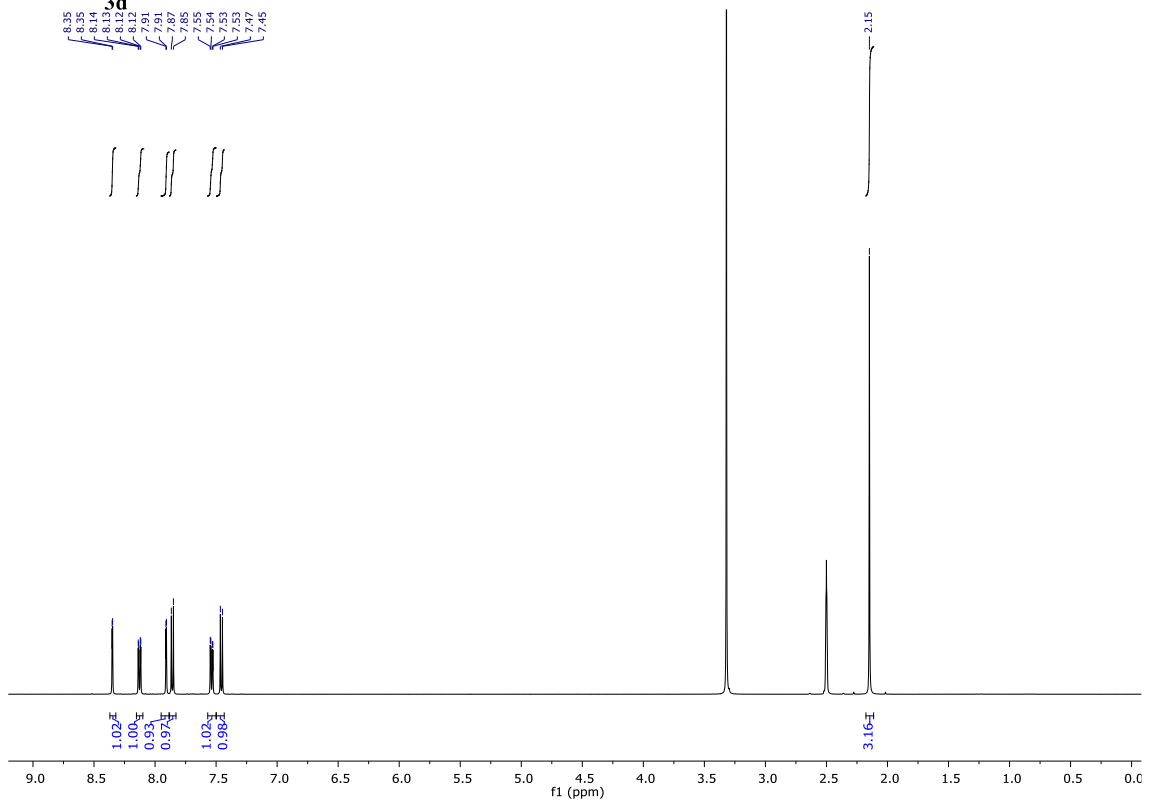
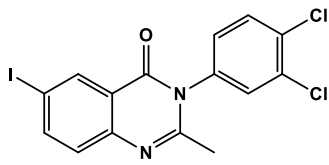
Spectrum



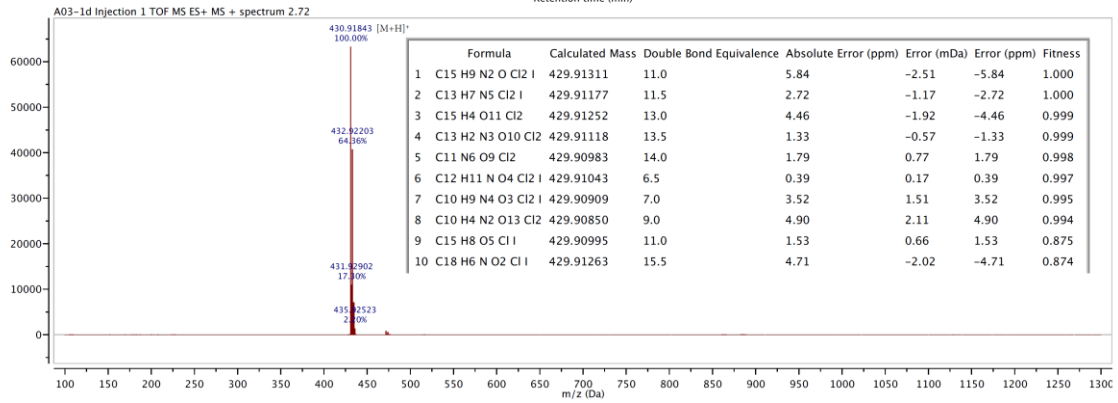
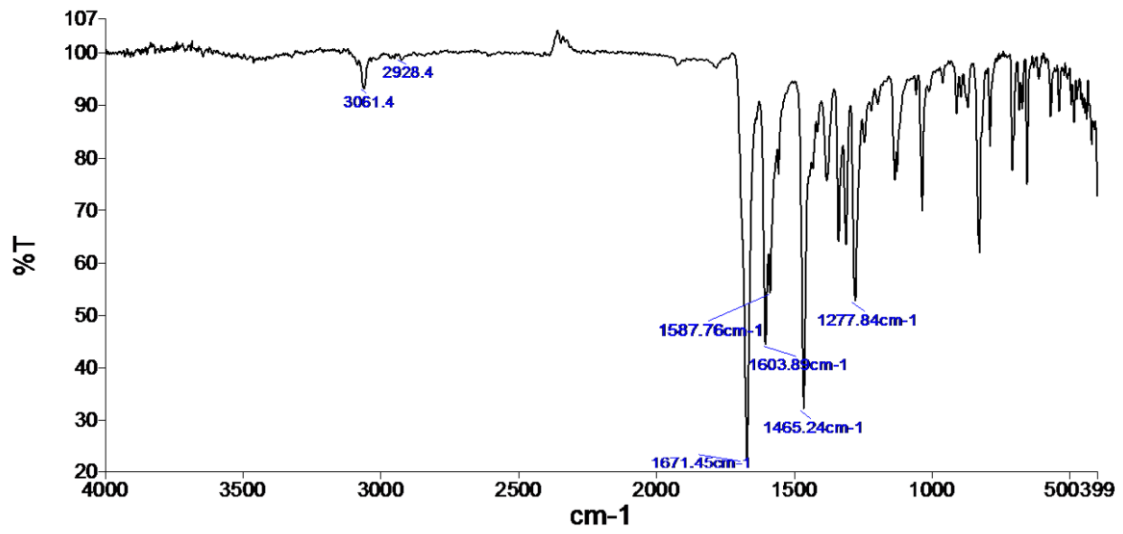


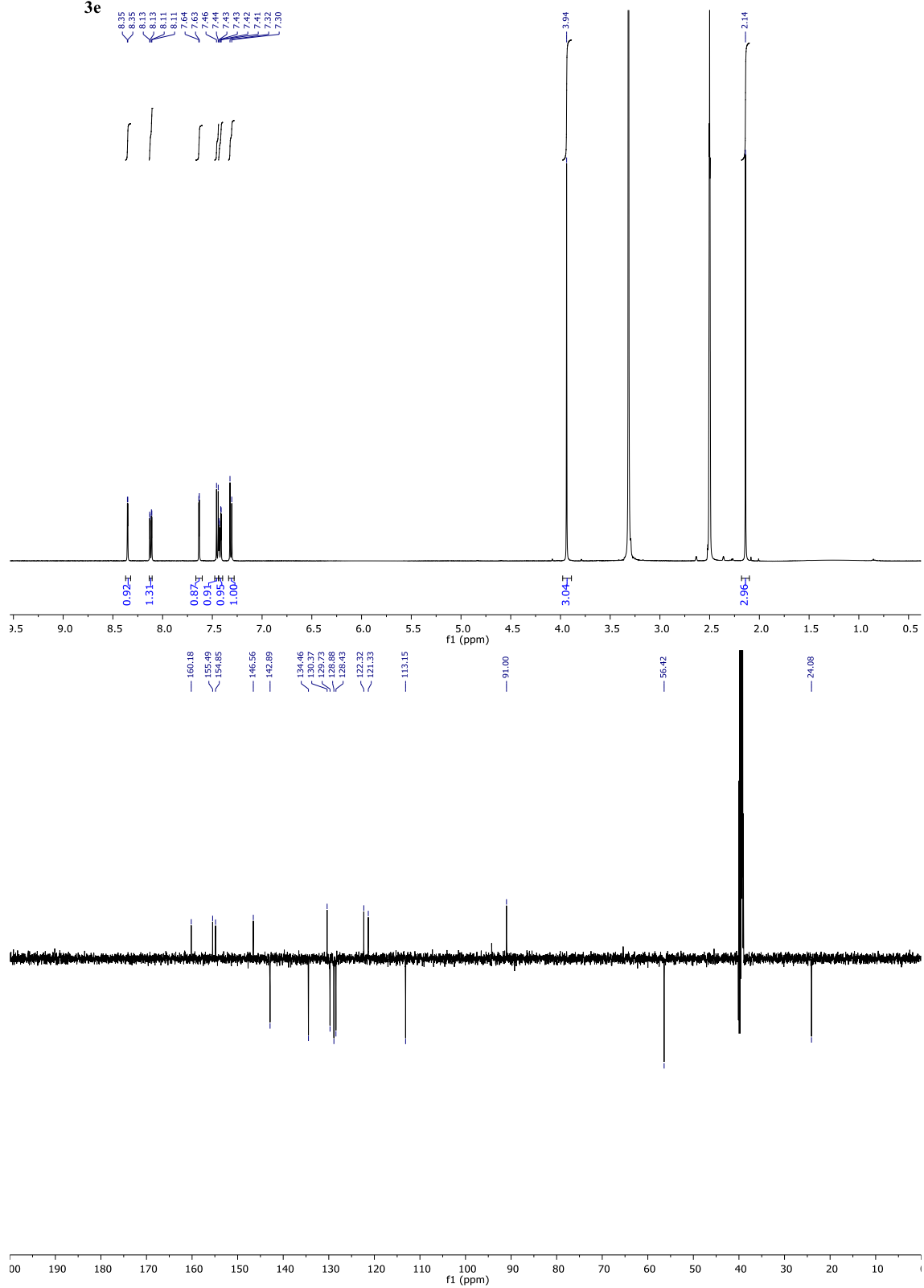
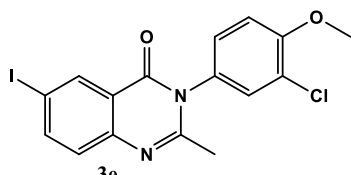
Spectrum



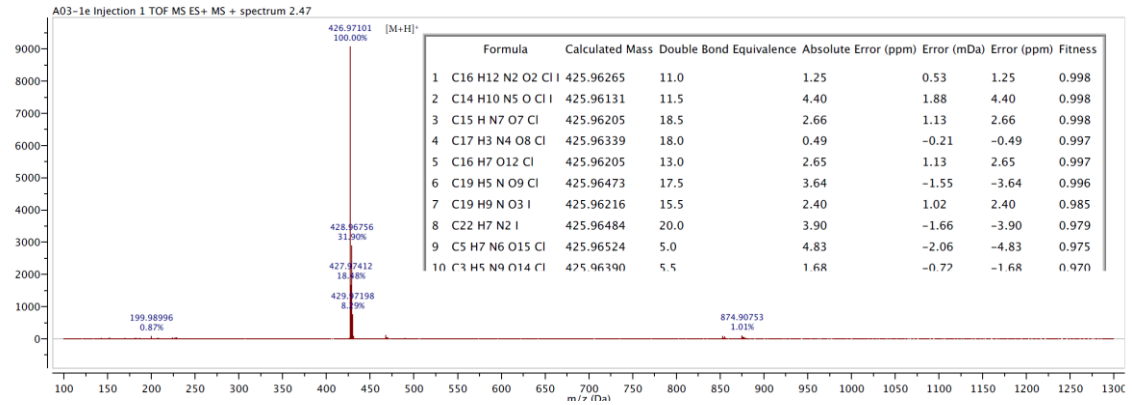
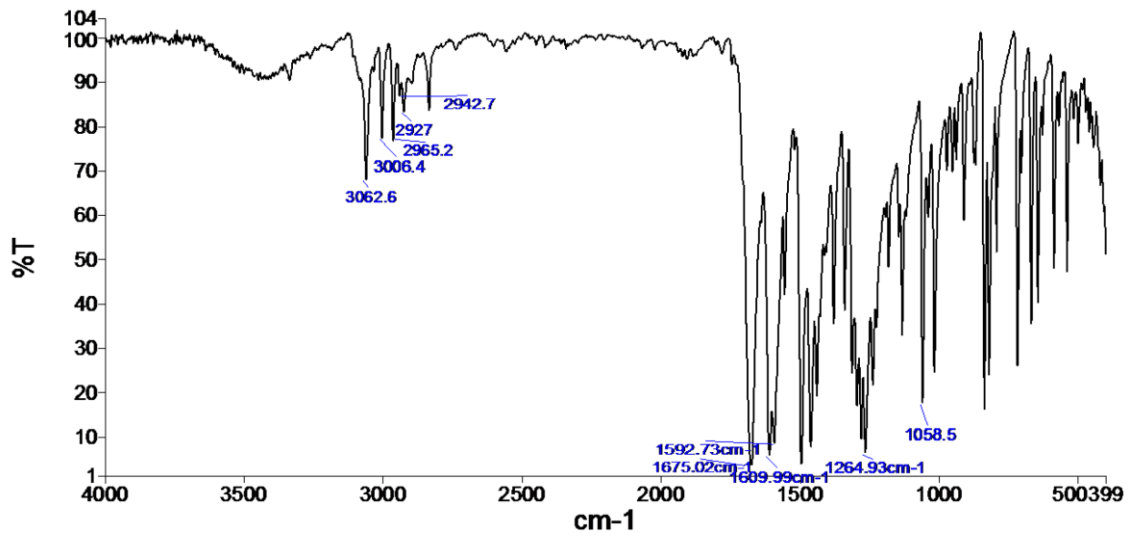


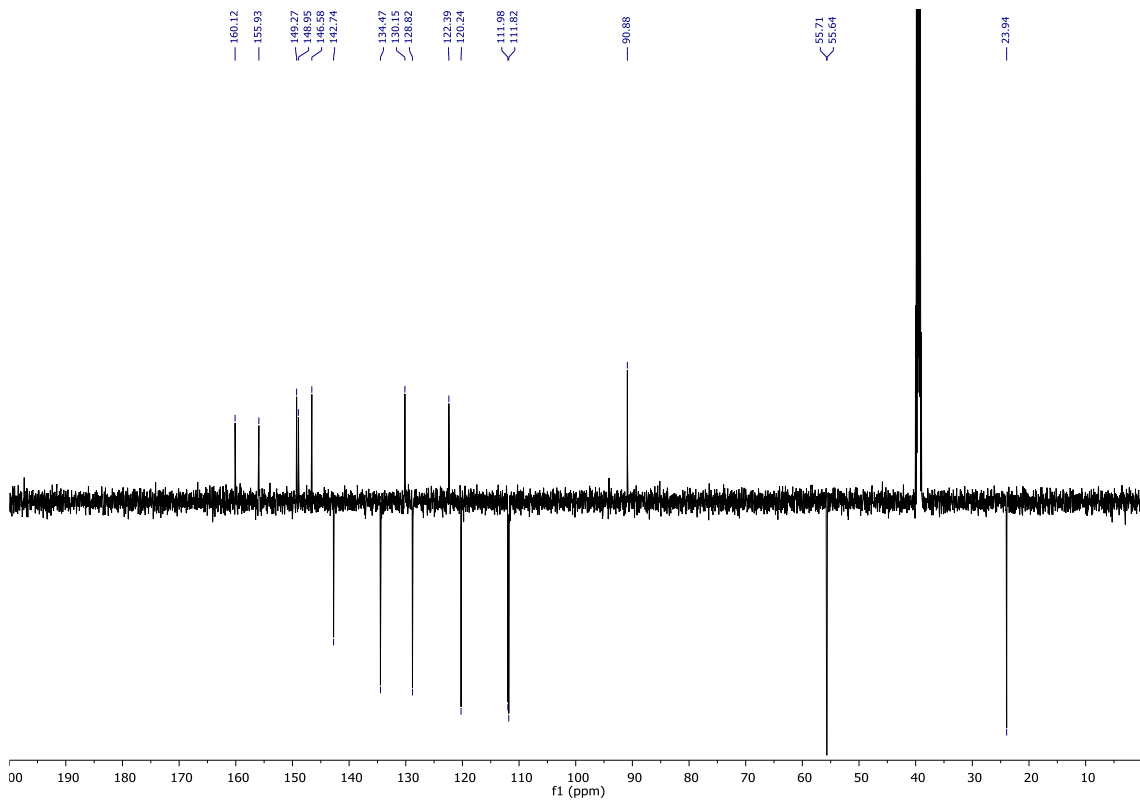
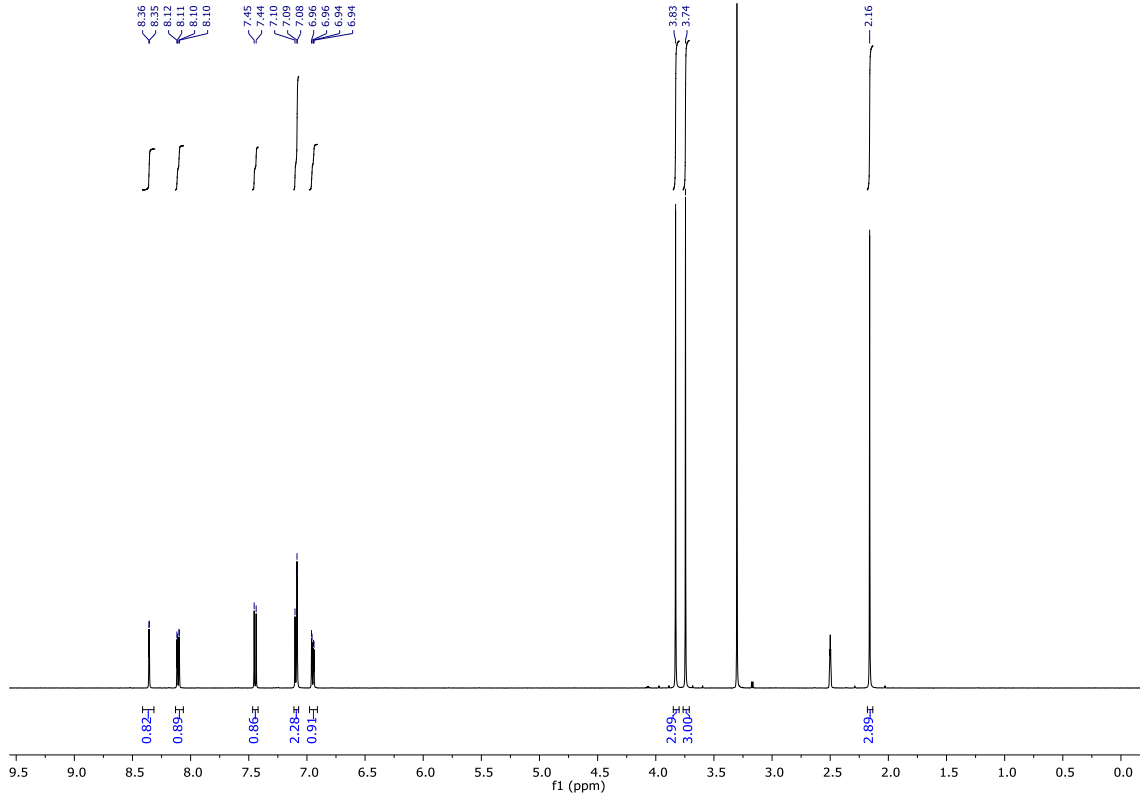
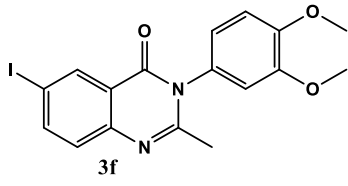
Spectrum



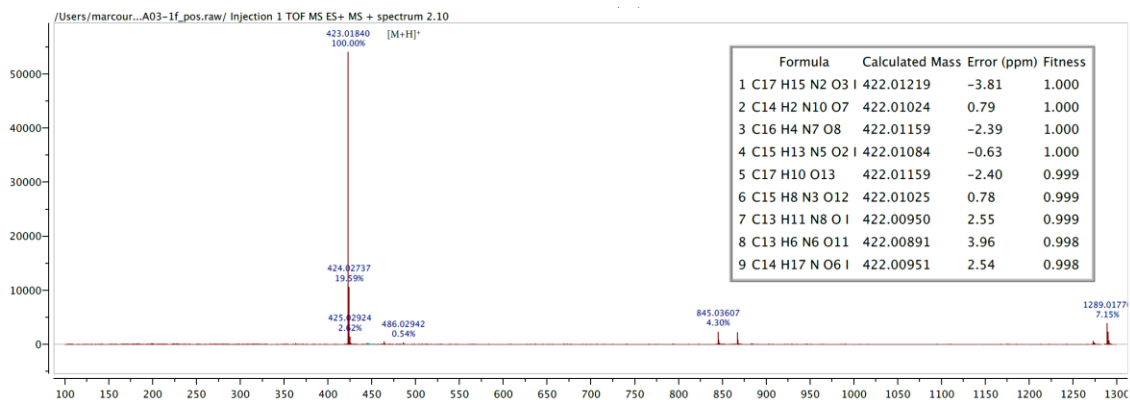
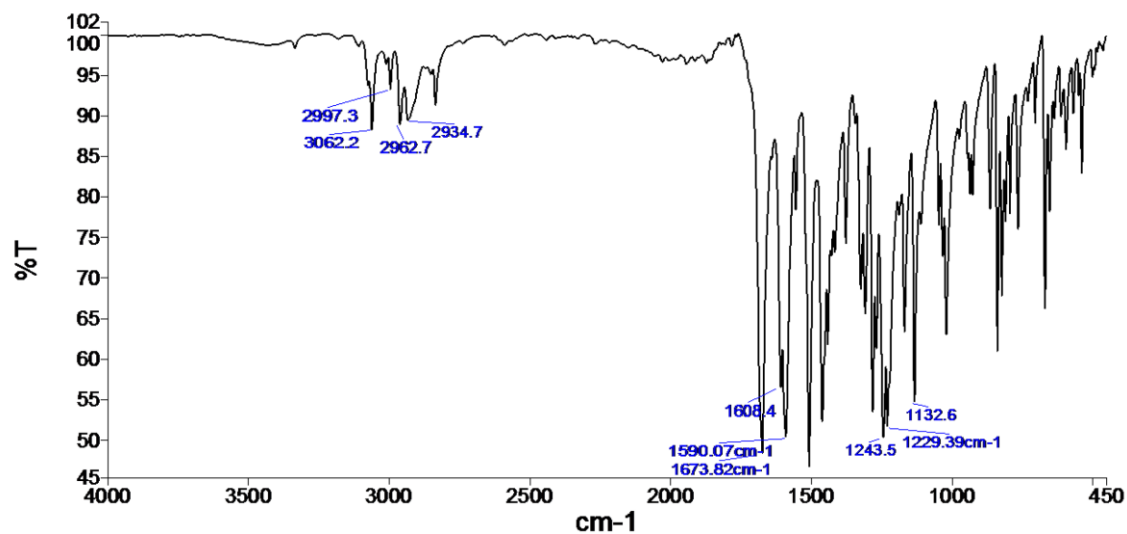


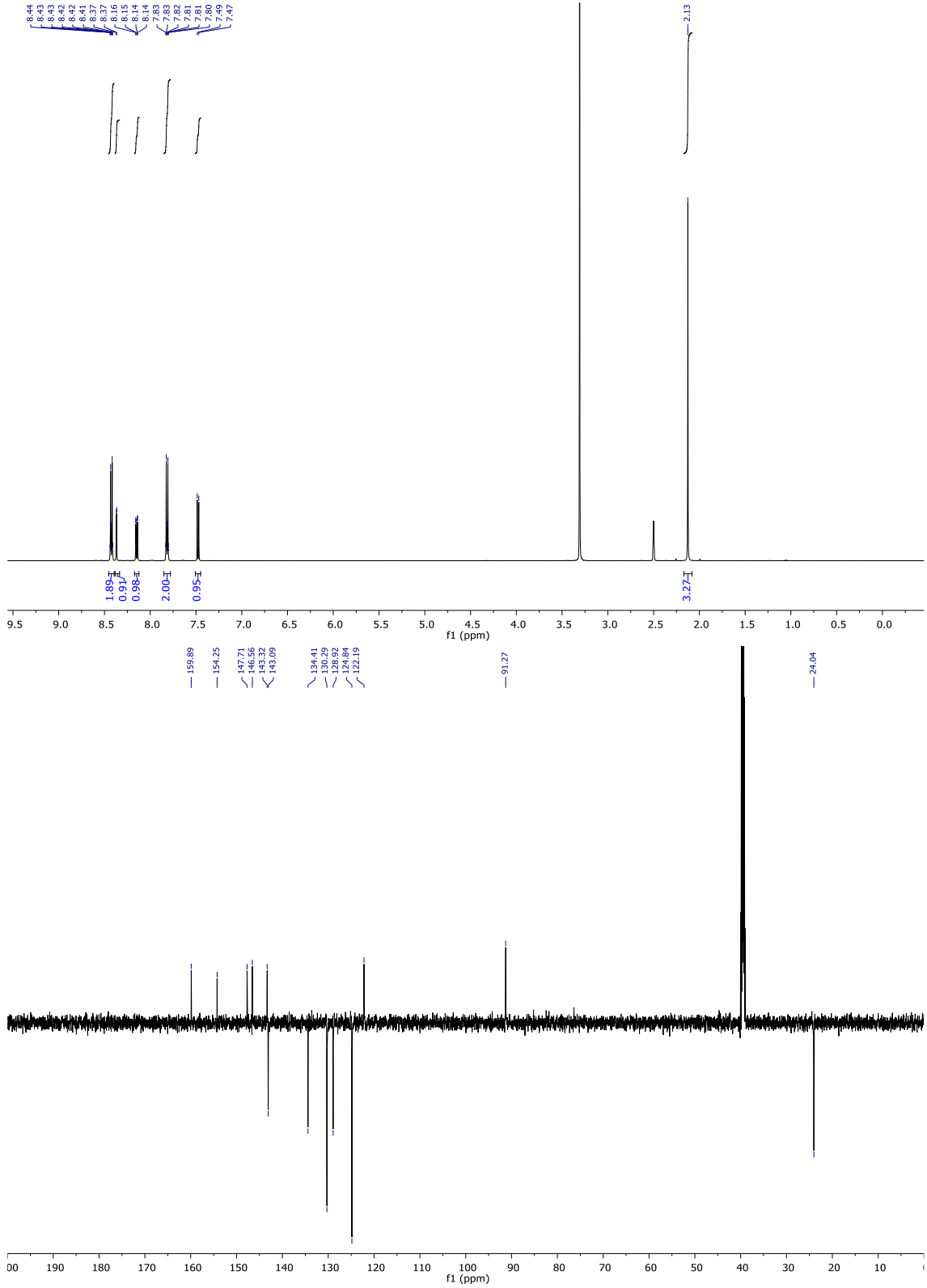
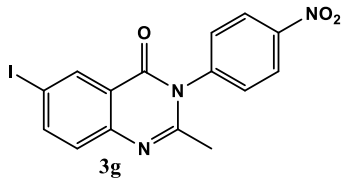
Spectrum



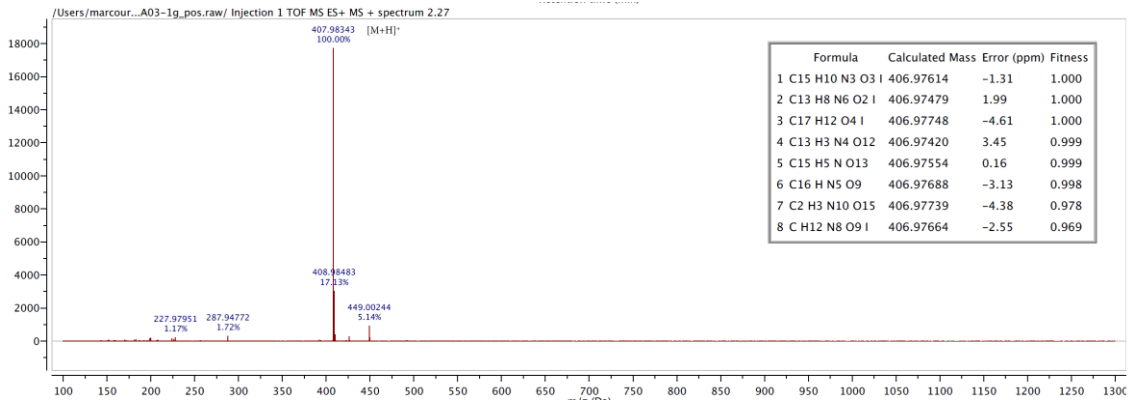
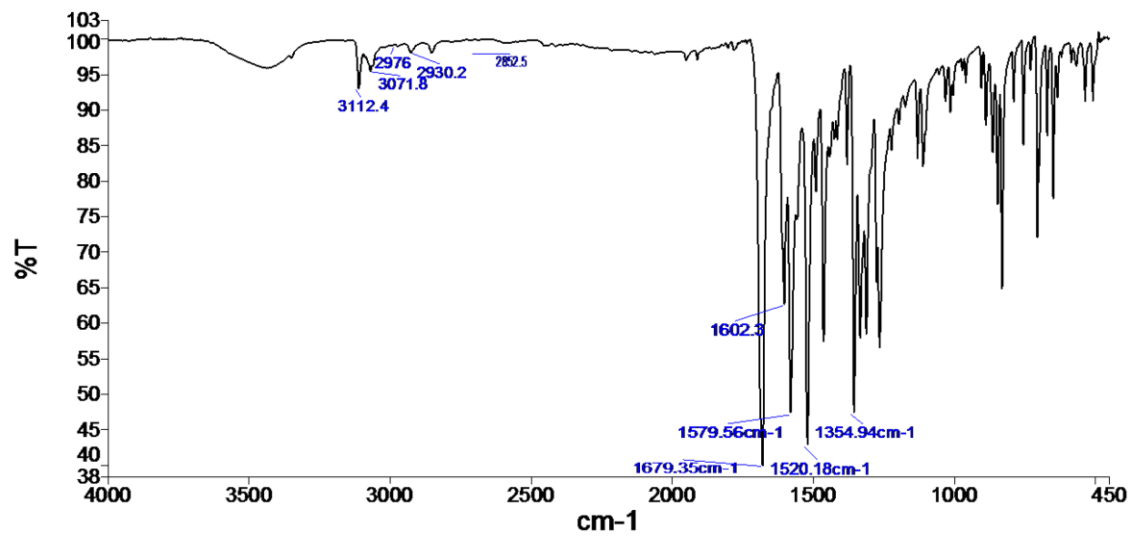


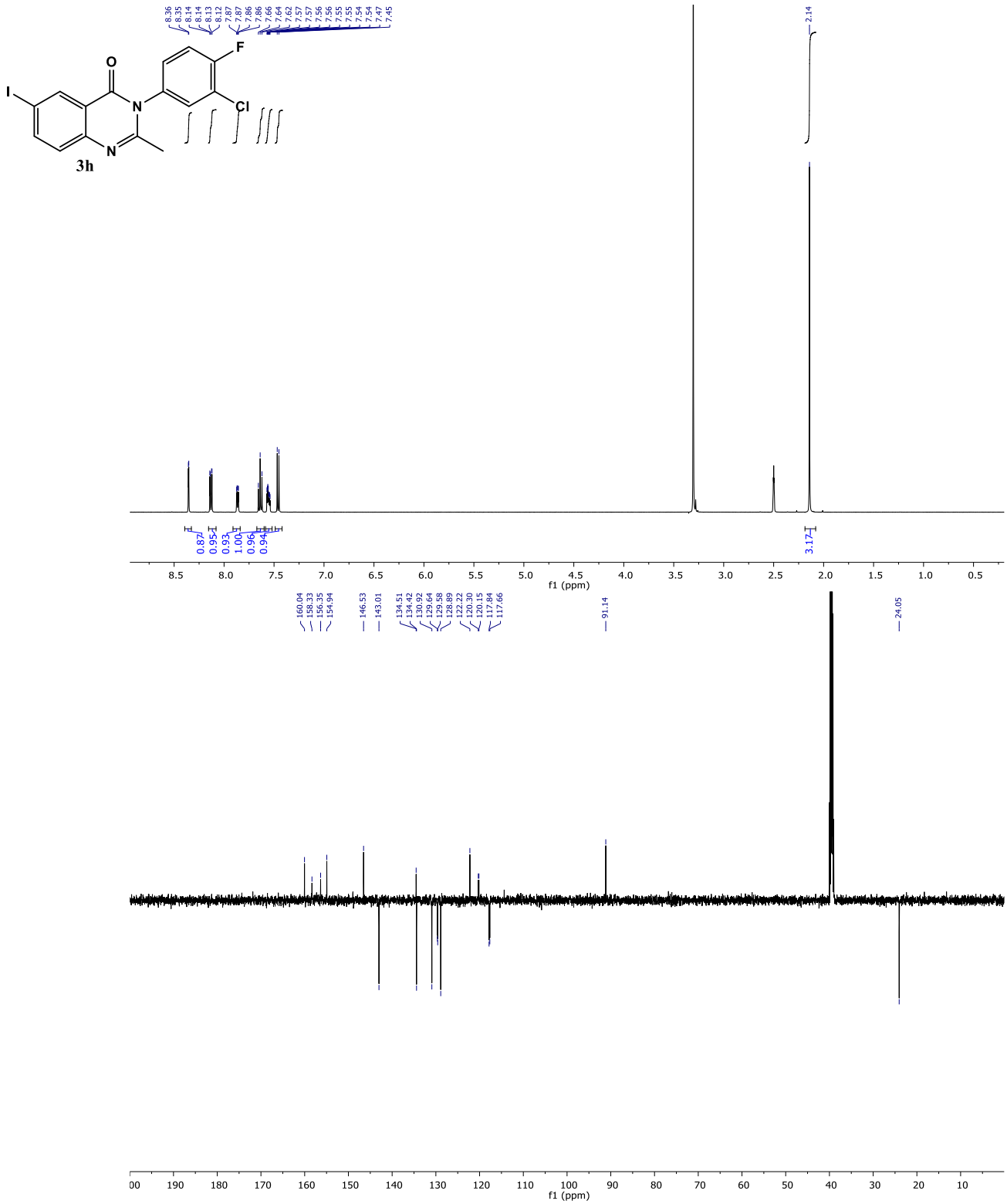
Spectrum



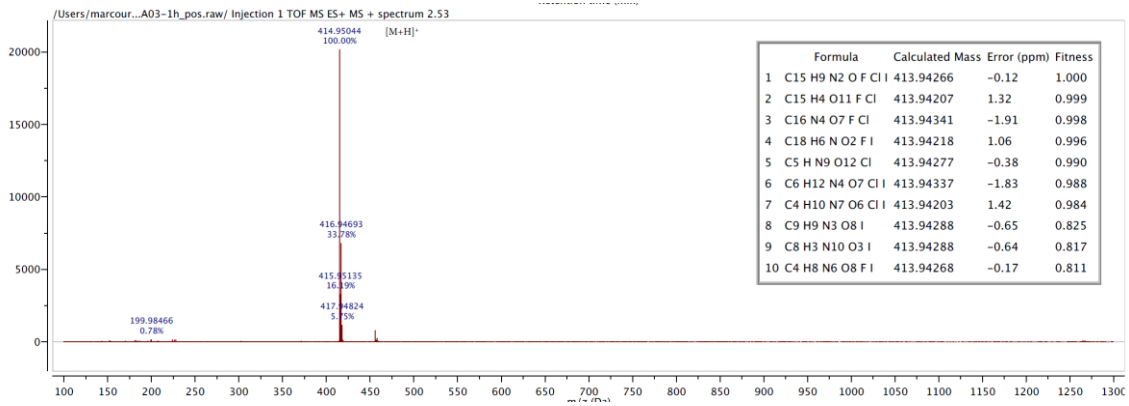
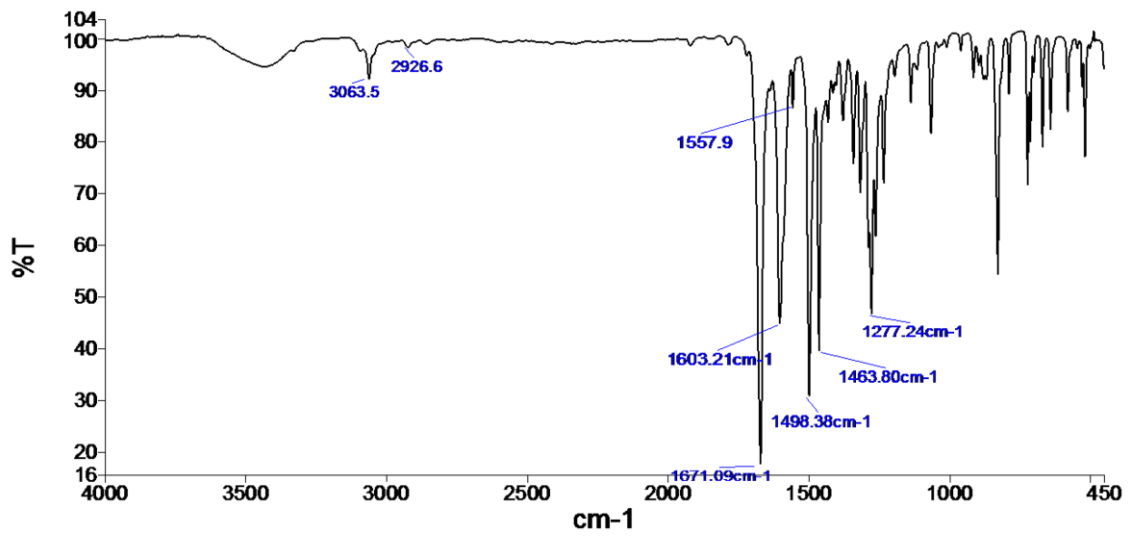


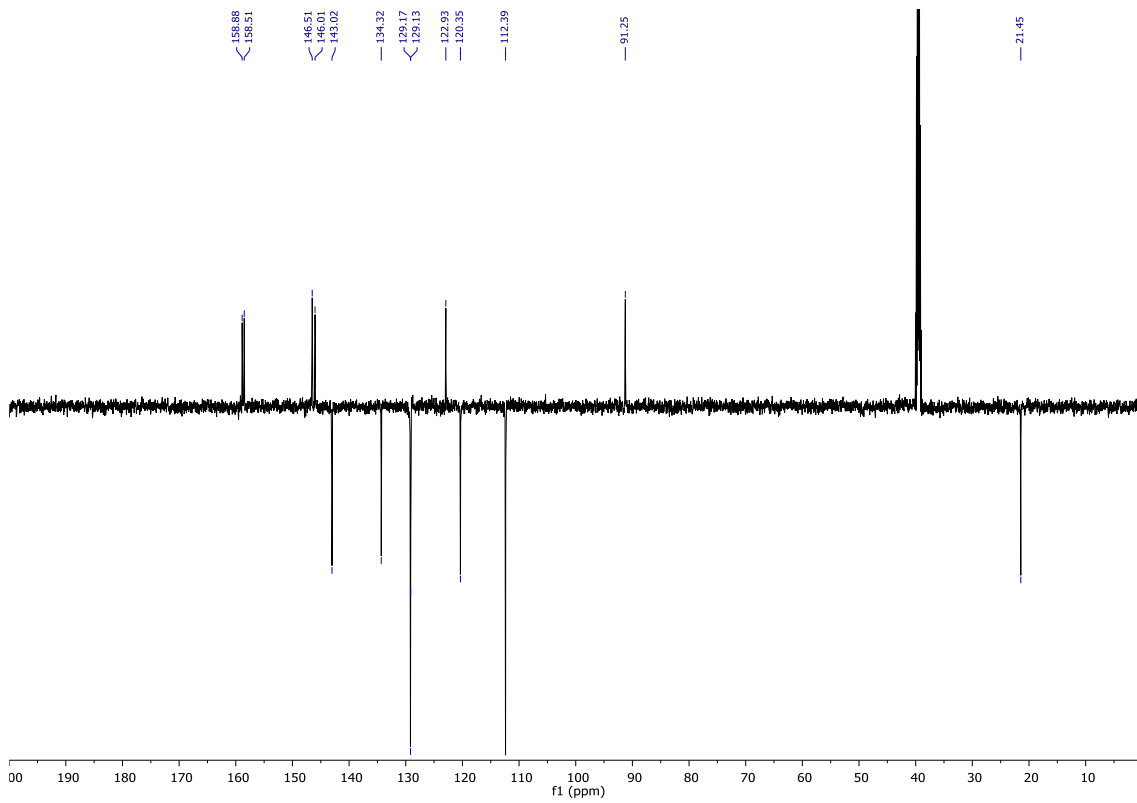
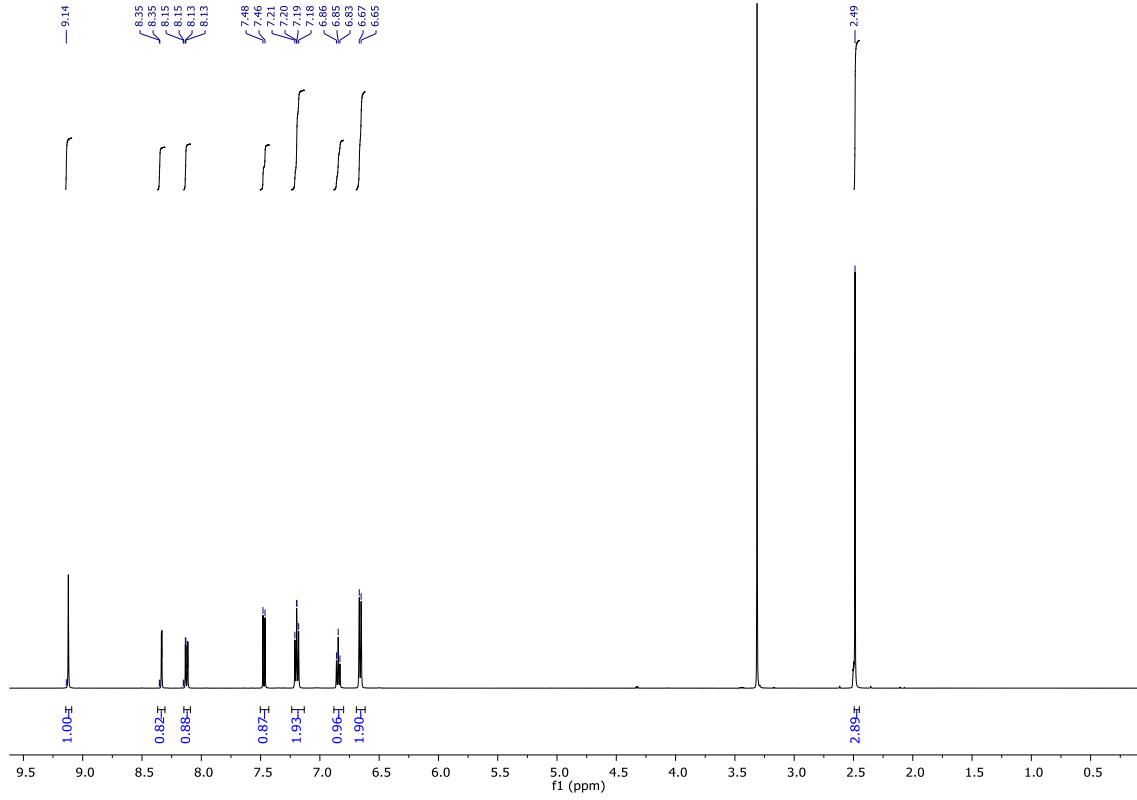
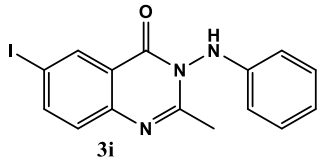
Spectrum



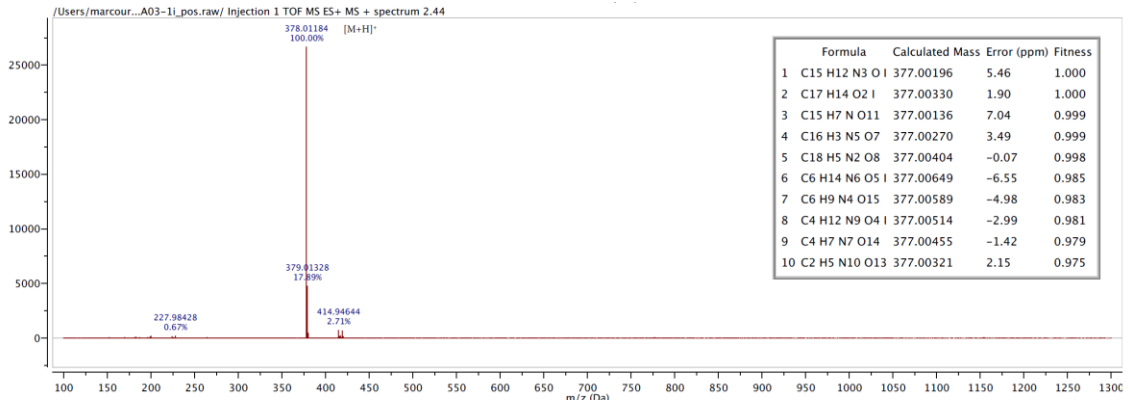
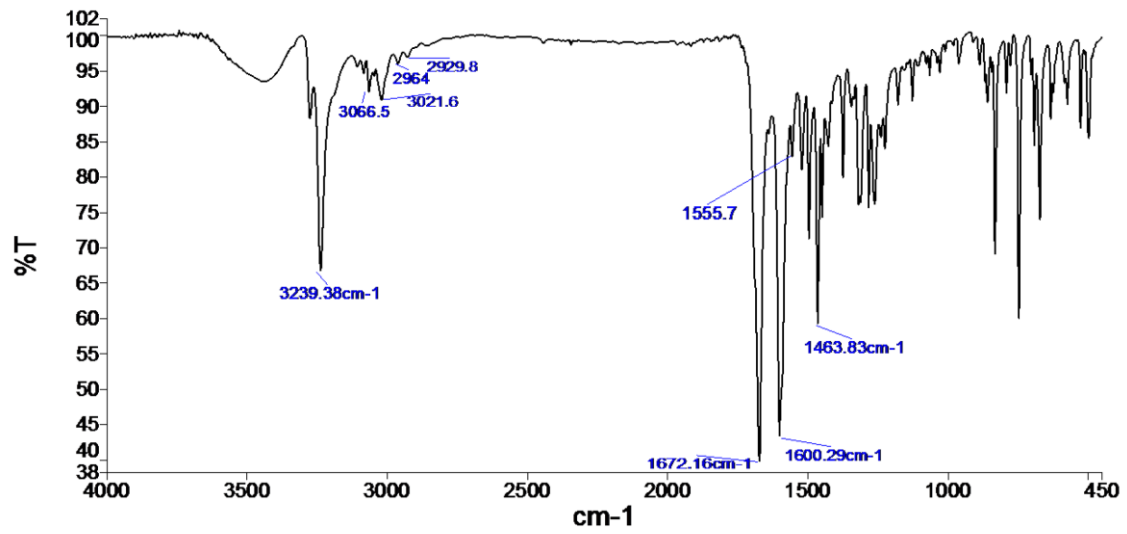


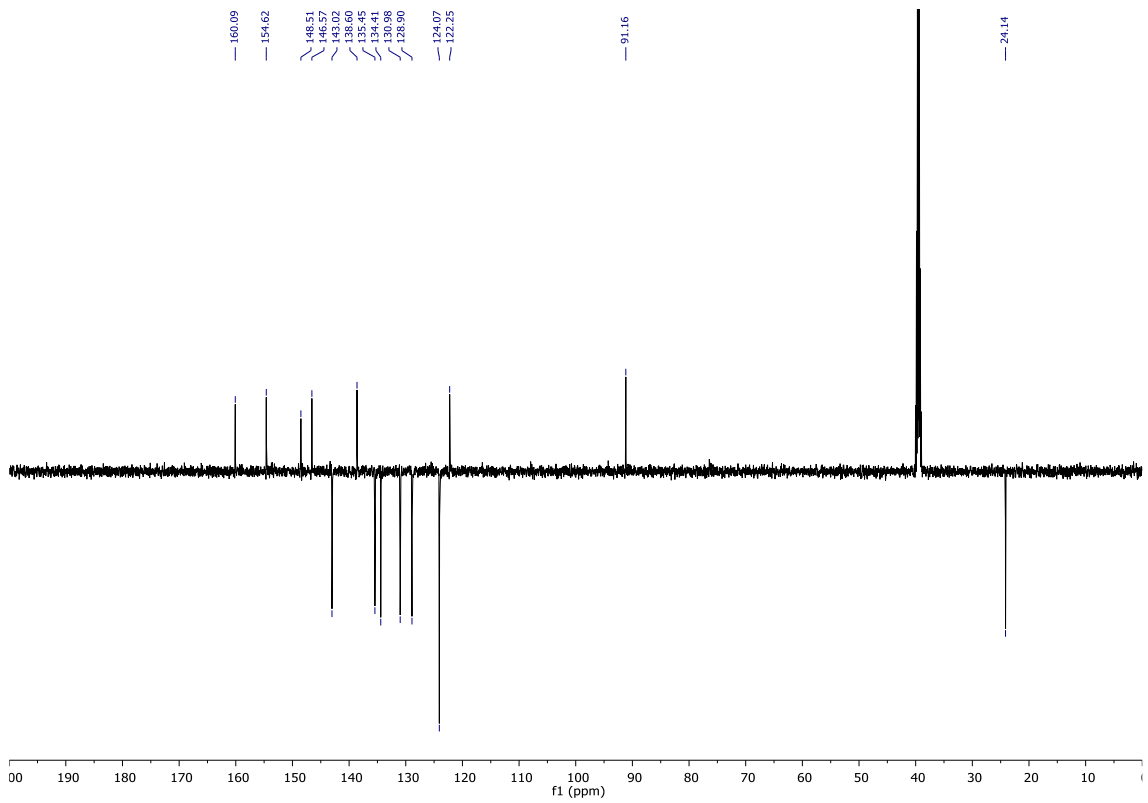
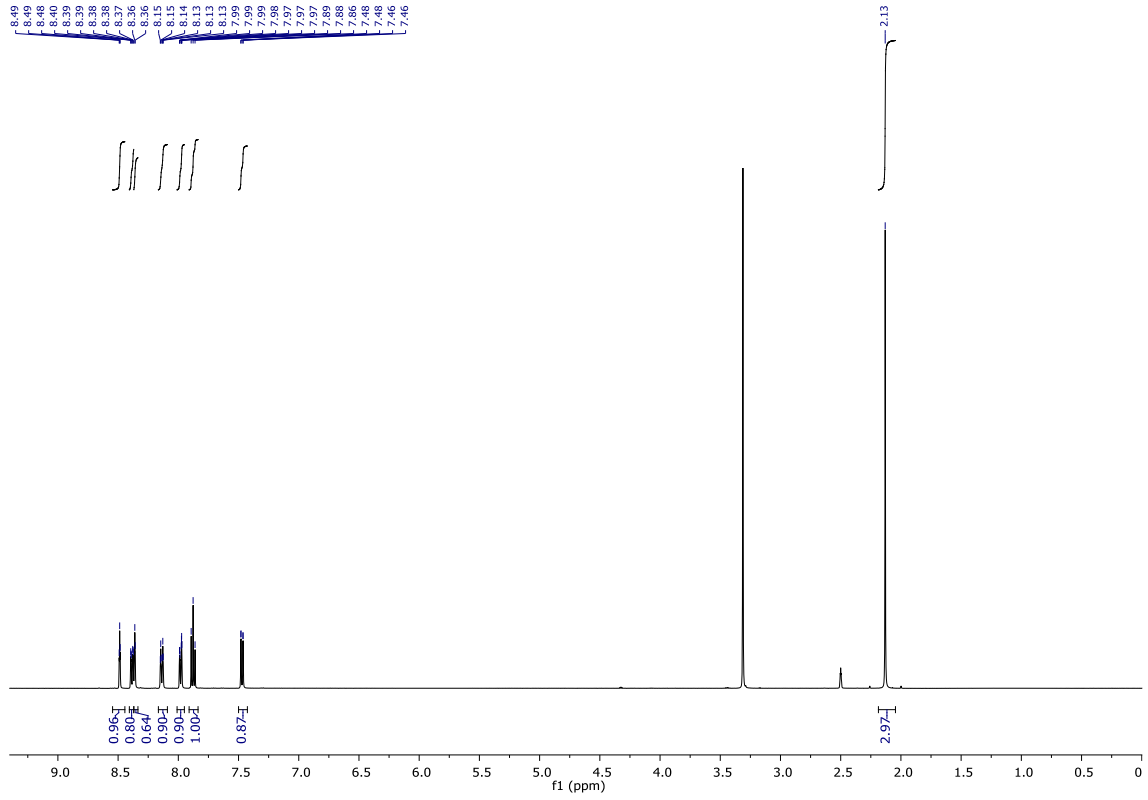
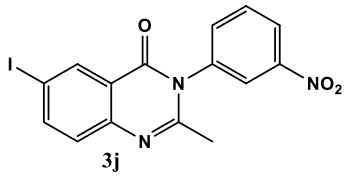
Spectrum



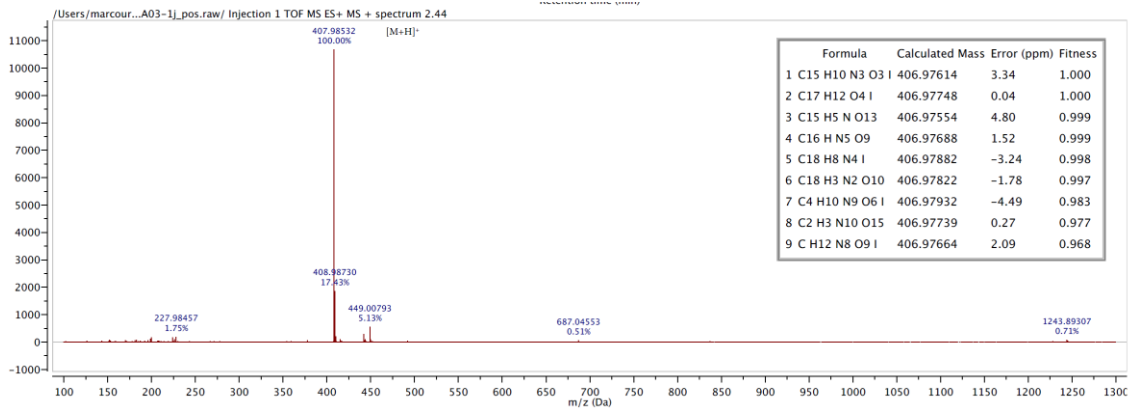
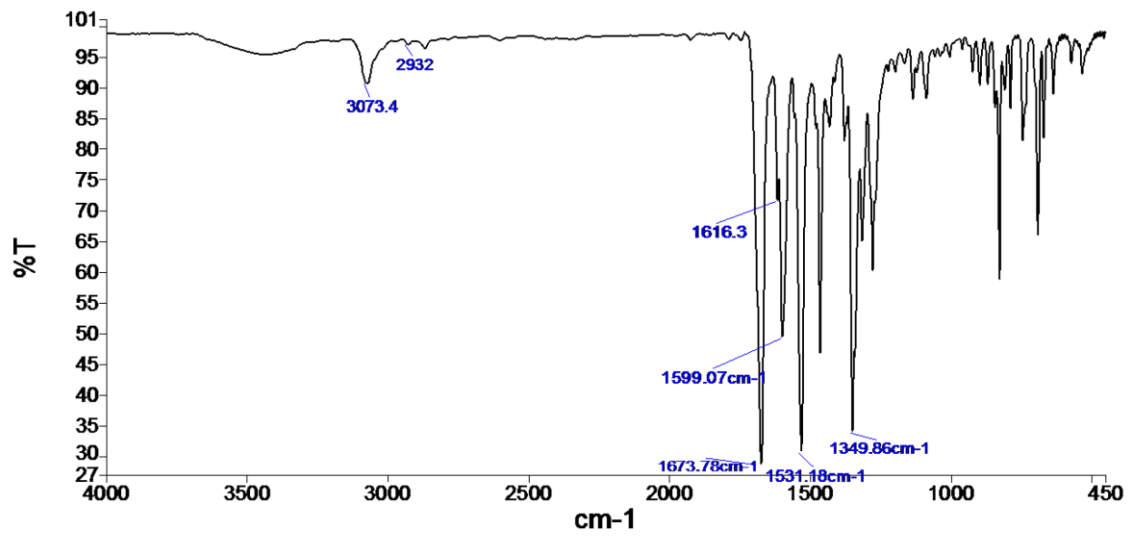


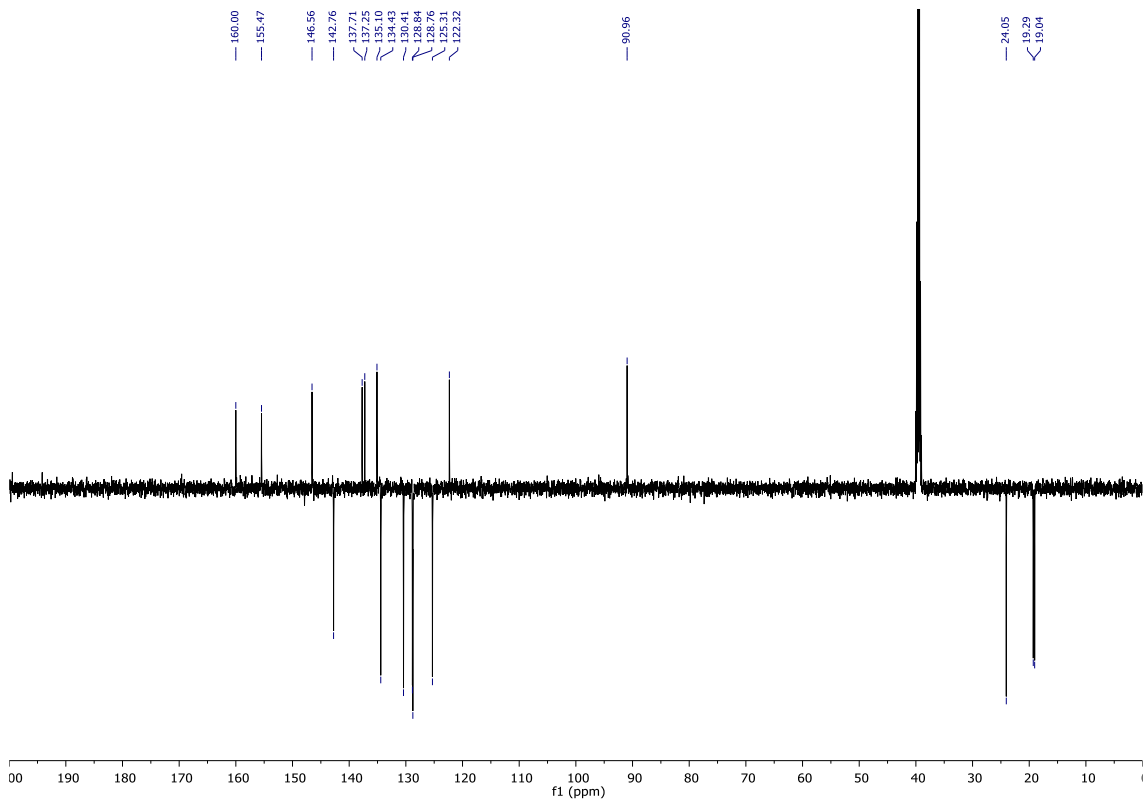
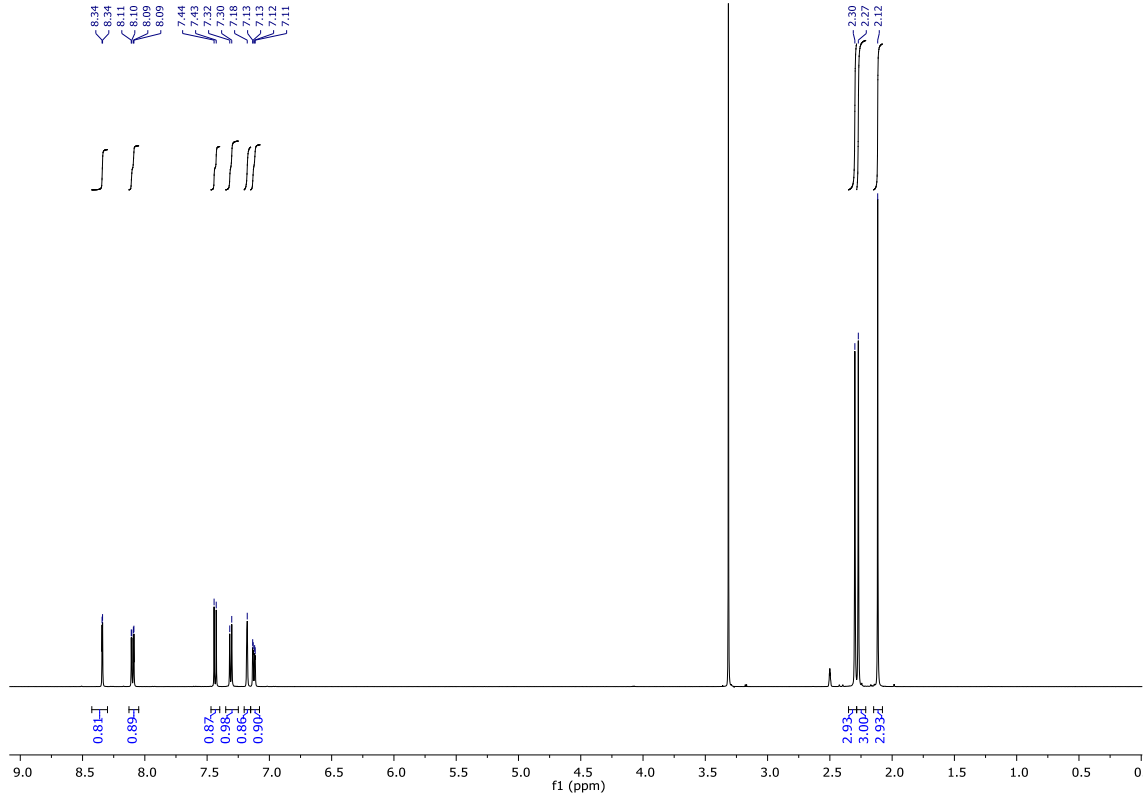
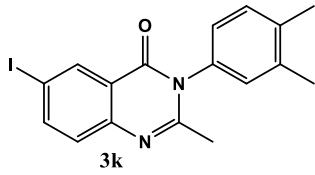
Spectrum



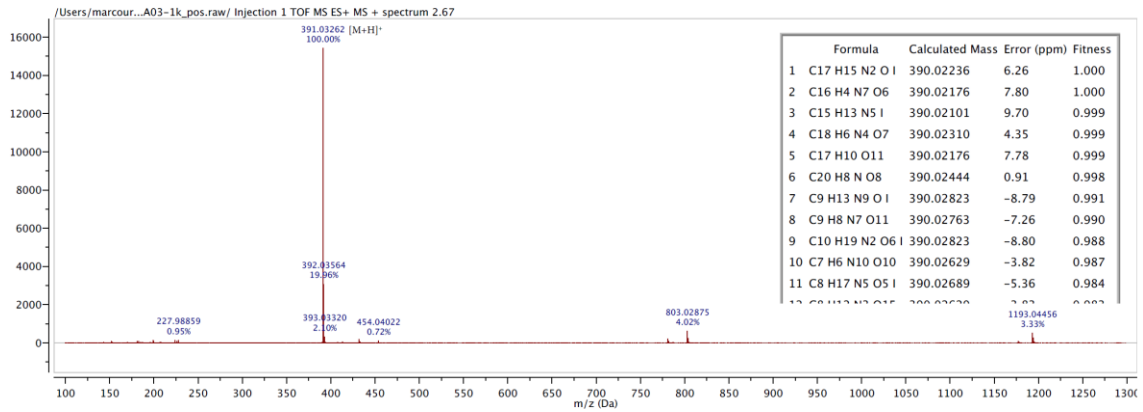
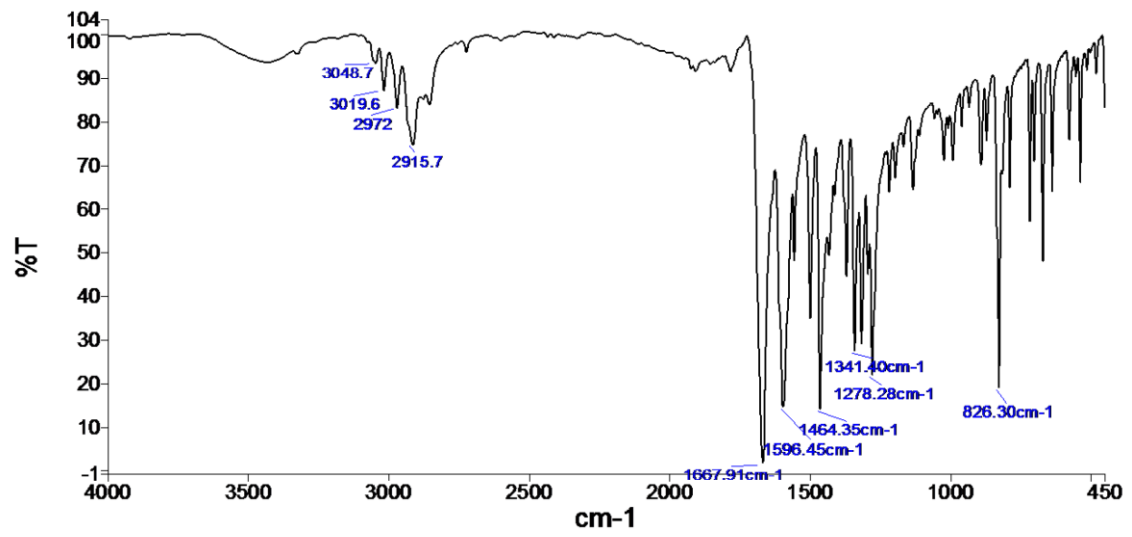


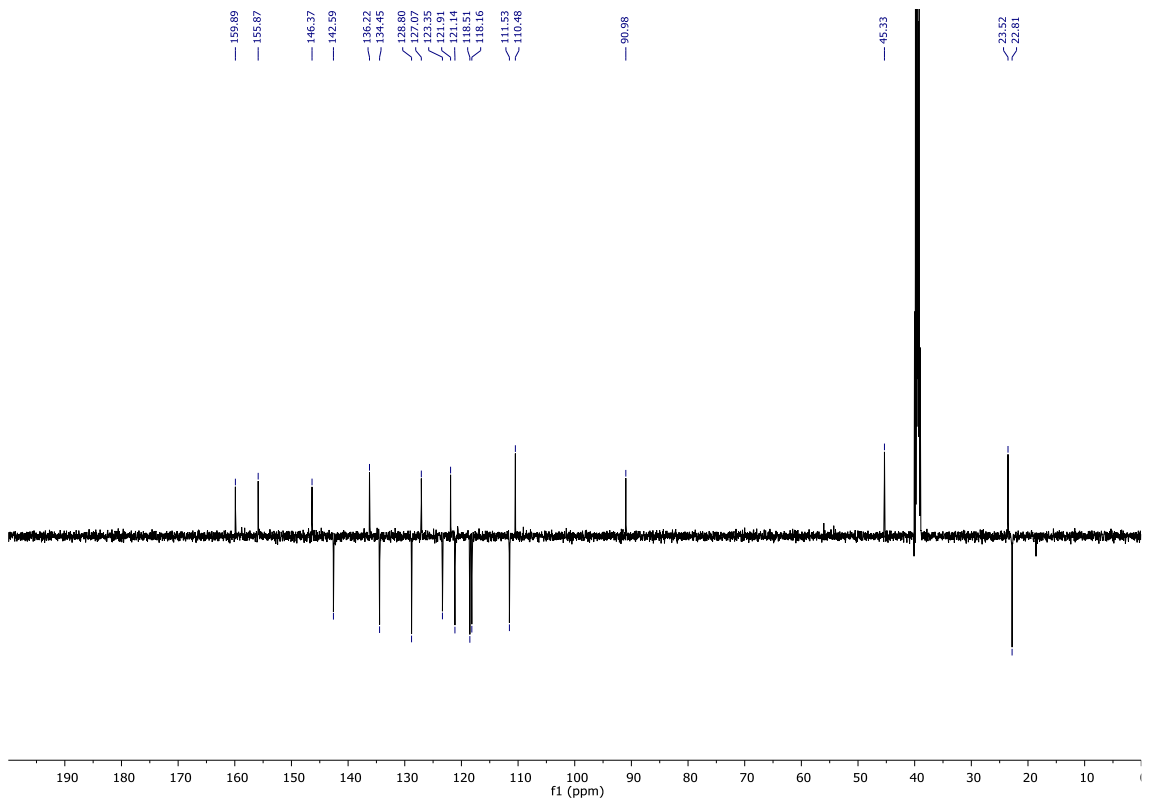
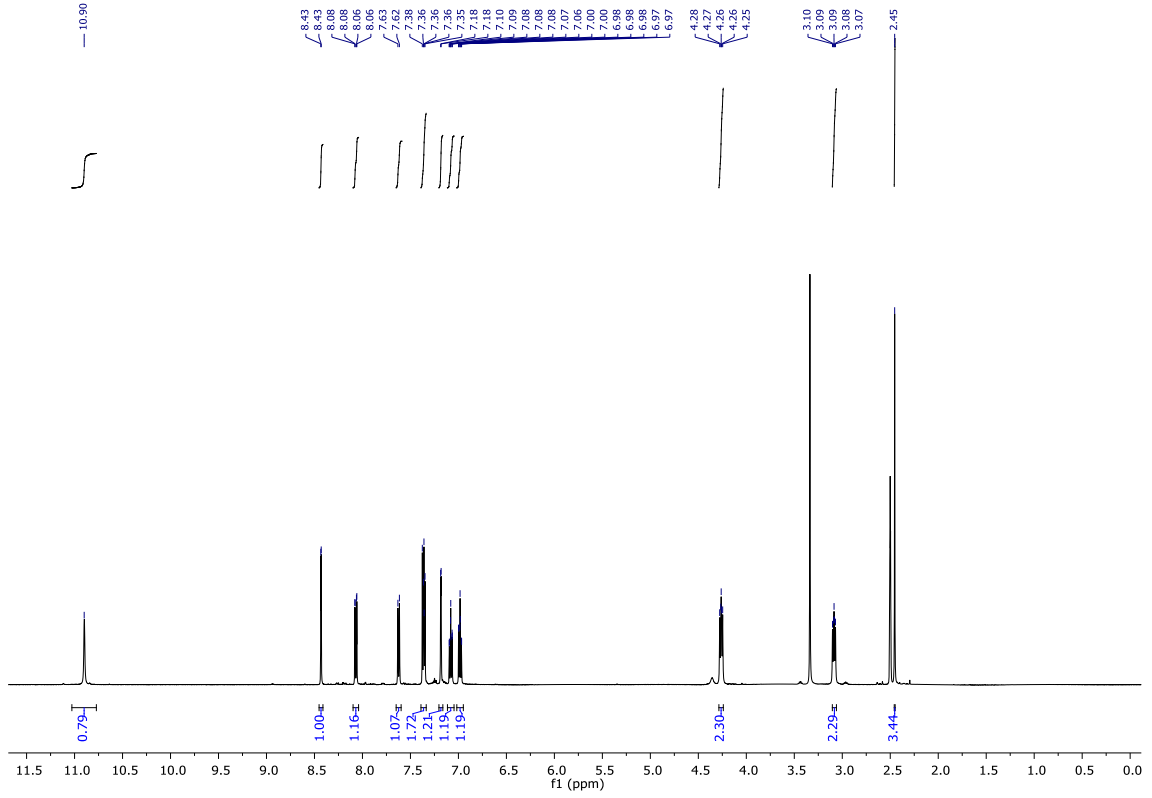
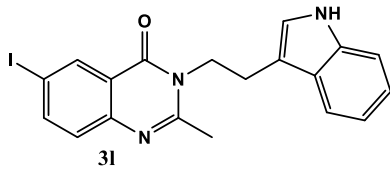
Spectrum



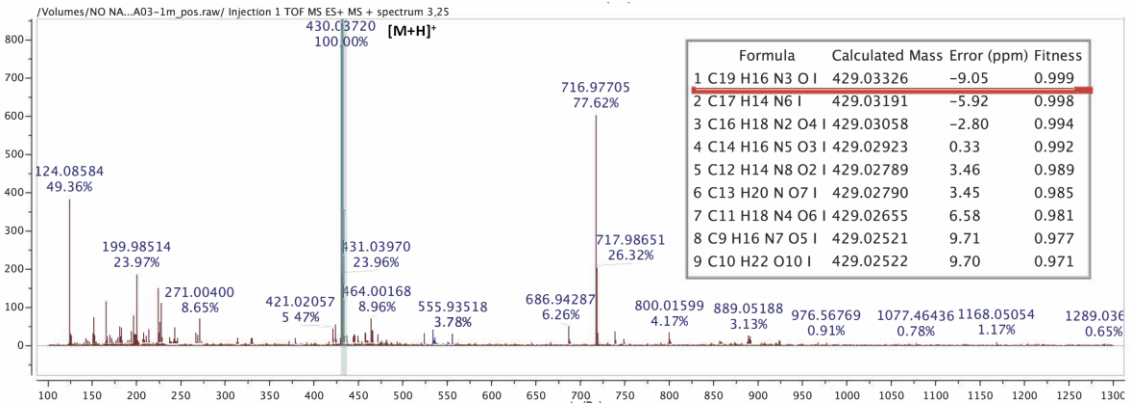
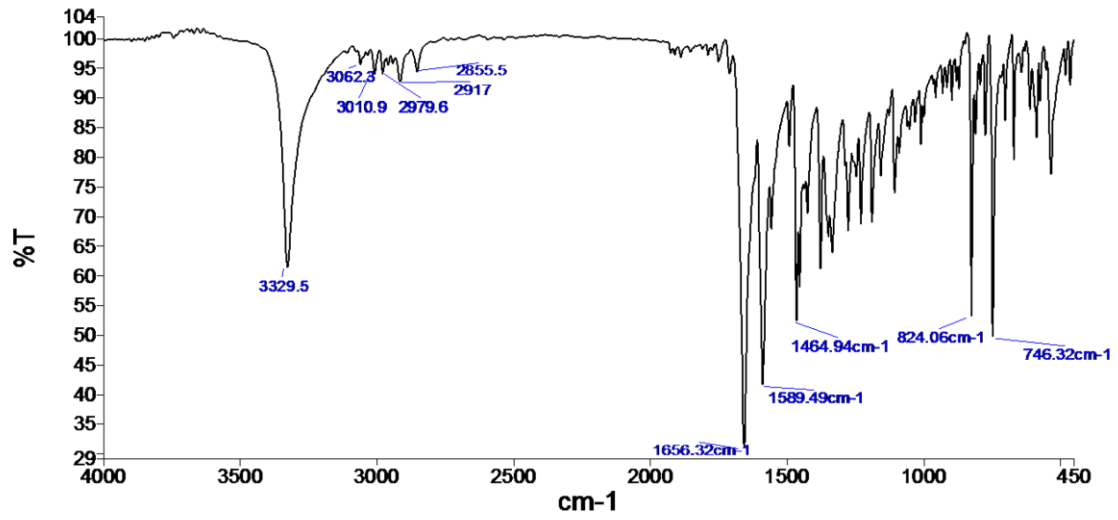


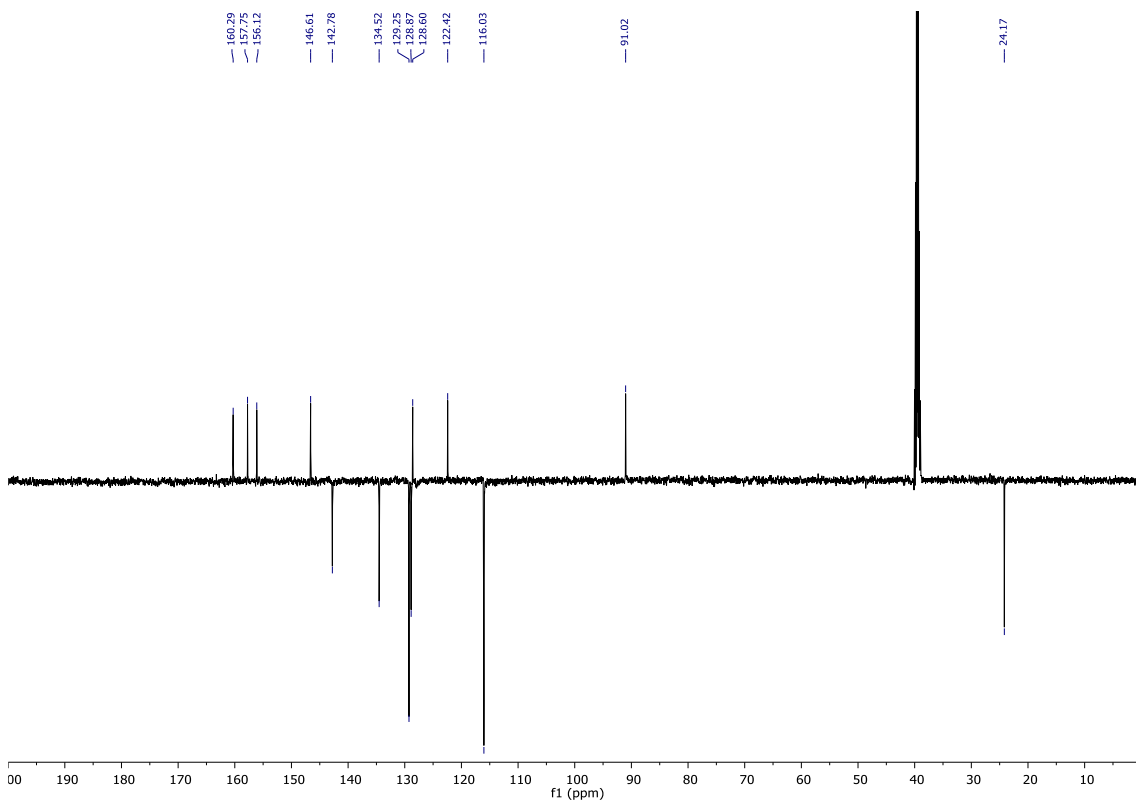
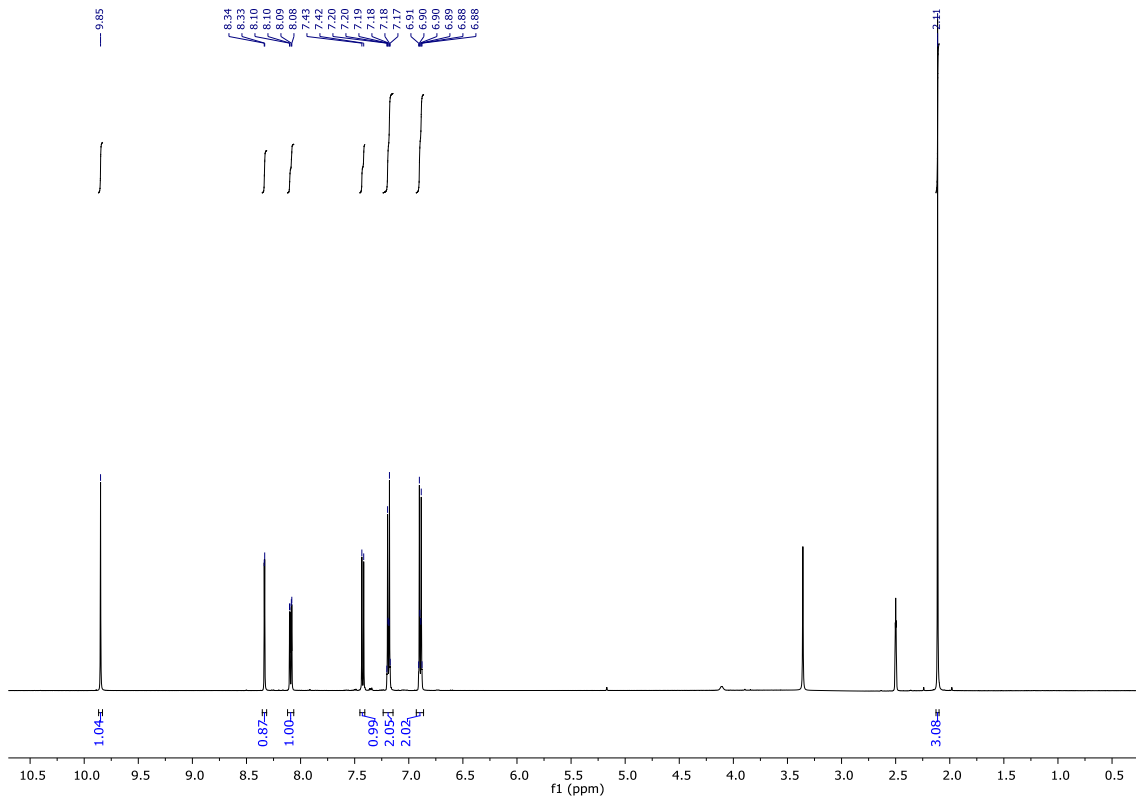
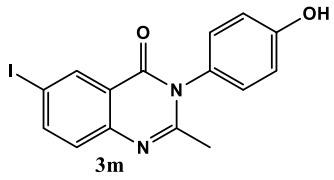
Spectrum



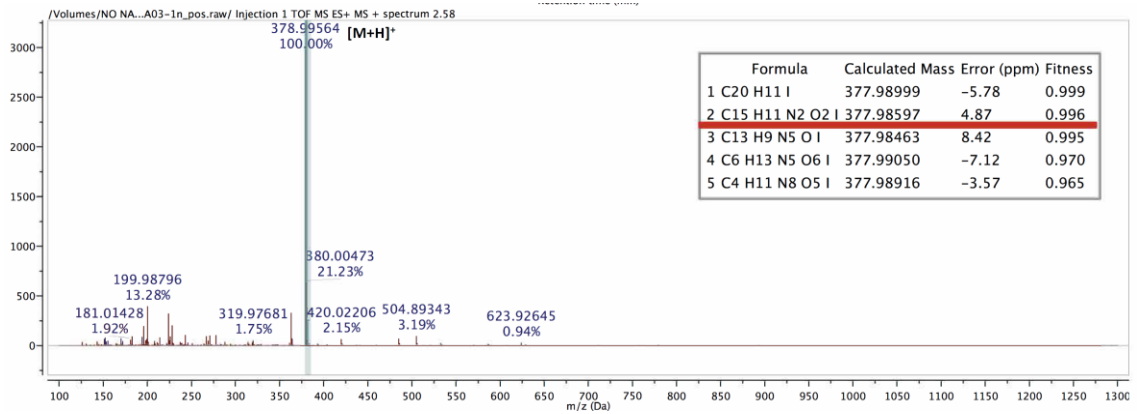
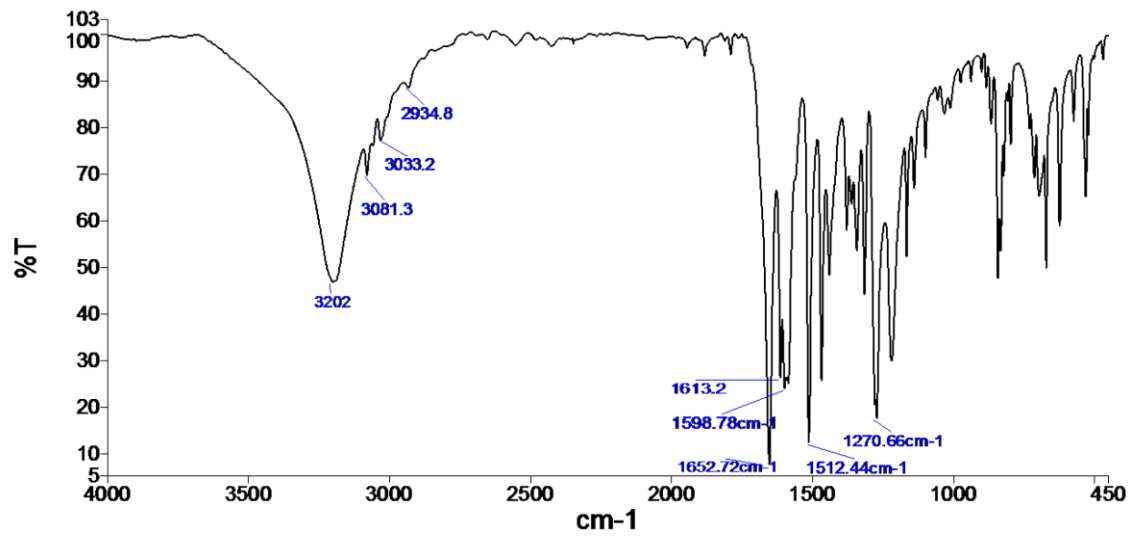


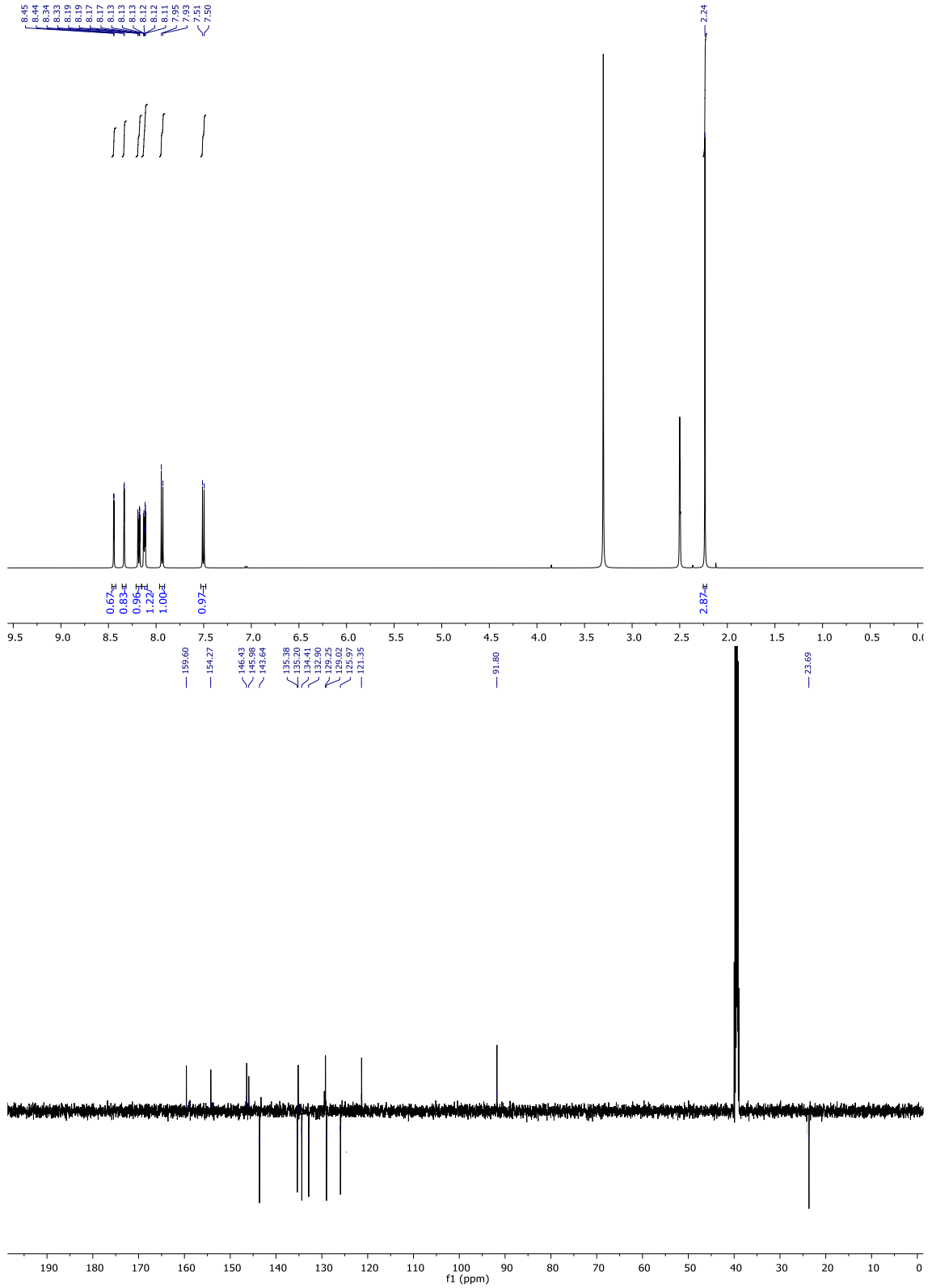
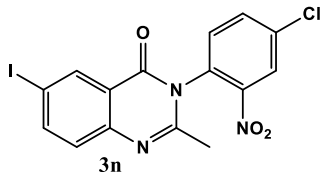
Spectrum





Spectrum





Spectrum

